SERALD - A SECCHI EUVI Ridge And Loop Detection tool

Bernd Inhester, Li Feng, Borut Podlipnik

Max Planck Institute
for Solar System Research

We benfit from discussions with the ISSI working group, in particular with Jean-Francois Hochedez and Thierry DuDoc de Wit.

The problem of extracting essential information out of digital images is shared with many other diciplines:

- medical imaging
- aerial photography
- ...

The problem of extracting essential information out of digital images is shared with many other diciplines:

- medical imaging
- aerial photography
- ...

Alternative approaches to the one presented here:

- Ridgelets (straight), curvelets

The problem of extracting essential information out of digital images is shared with many other diciplines:

- medical imaging
- aerial photography
- . . .

Alternative approaches to the one presented here:

- Ridgelets (straight), curvelets
- Watershet segmentation, yields always closed curves

The problem of extracting essential information out of digital images is shared with many other diciplines:

- medical imaging
- aerial photography
- ...

Alternative approaches to the one presented here:

- Ridgelets (straight), curvelets
- Watershet segmentation, yields always closed curves
- Principle curves, needs to be extended from dots to pixels

The problem of extracting essential information out of digital images is shared with many other diciplines:

- medical imaging
- aerial photography
- ...

Alternative approaches to the one presented here:

- Ridgelets (straight), curvelets
- Watershet segmentation, yields always closed curves
- Principle curves, needs to be extended from dots to pixels
- Tensor voting, a method to connect ridge points

The problem of extracting essential information out of digital images is shared with many other diciplines:

- medical imaging
- aerial photography
- . . .

Alternative approaches to the one presented here:

- Ridgelets (straight), curvelets
- Watershet segmentation, yields always closed curves
- Principle curves, needs to be extended from dots to pixels
- Tensor voting, a method to connect ridge points
- . . .

In solar physics, odd-order image filters are quite popular, they are good for edges, but yield wrong loop postions.

$\Rightarrow$ need local Taylor series expansion to at least 2nd order

$$I_{\mathrm{approx}}(\boldsymbol{x}) \simeq I(\boldsymbol{i}) + \boldsymbol{g}^T(\boldsymbol{x}-\boldsymbol{i}) + (\boldsymbol{x}-\boldsymbol{i})^T \boldsymbol{H}\ (\boldsymbol{x}-\boldsymbol{i})$$

$\boldsymbol{H}$ gives important information about the local orientation of a loop.

In solar physics, odd-order image filters are quite popular,
they are good for edges, but yield wrong loop postions.

$\Rightarrow$ need local Taylor series expansion to at least 2nd order

$$I_{\text{approx}}(\boldsymbol{x}) \simeq I(\boldsymbol{i}) + \boldsymbol{g}^T(\boldsymbol{x}-\boldsymbol{i}) + (\boldsymbol{x}-\boldsymbol{i})^T \boldsymbol{H}\,(\boldsymbol{x}-\boldsymbol{i})$$

$\boldsymbol{H}$ gives important information about the local orientation of a loop.

Strous et al. (200?) and Lee et al. (2006) use a 9-point stencil to estimate the Taylor coefficients.

Differentiation is ill-posed $\longrightarrow$ need for a properly regularised estimation for the Taylor coefficients.

1st step: Ridgel determination via Automated Scaling (Lindeberg, 1993)

For each image pixel we consider multiply sized neighbourhoods:

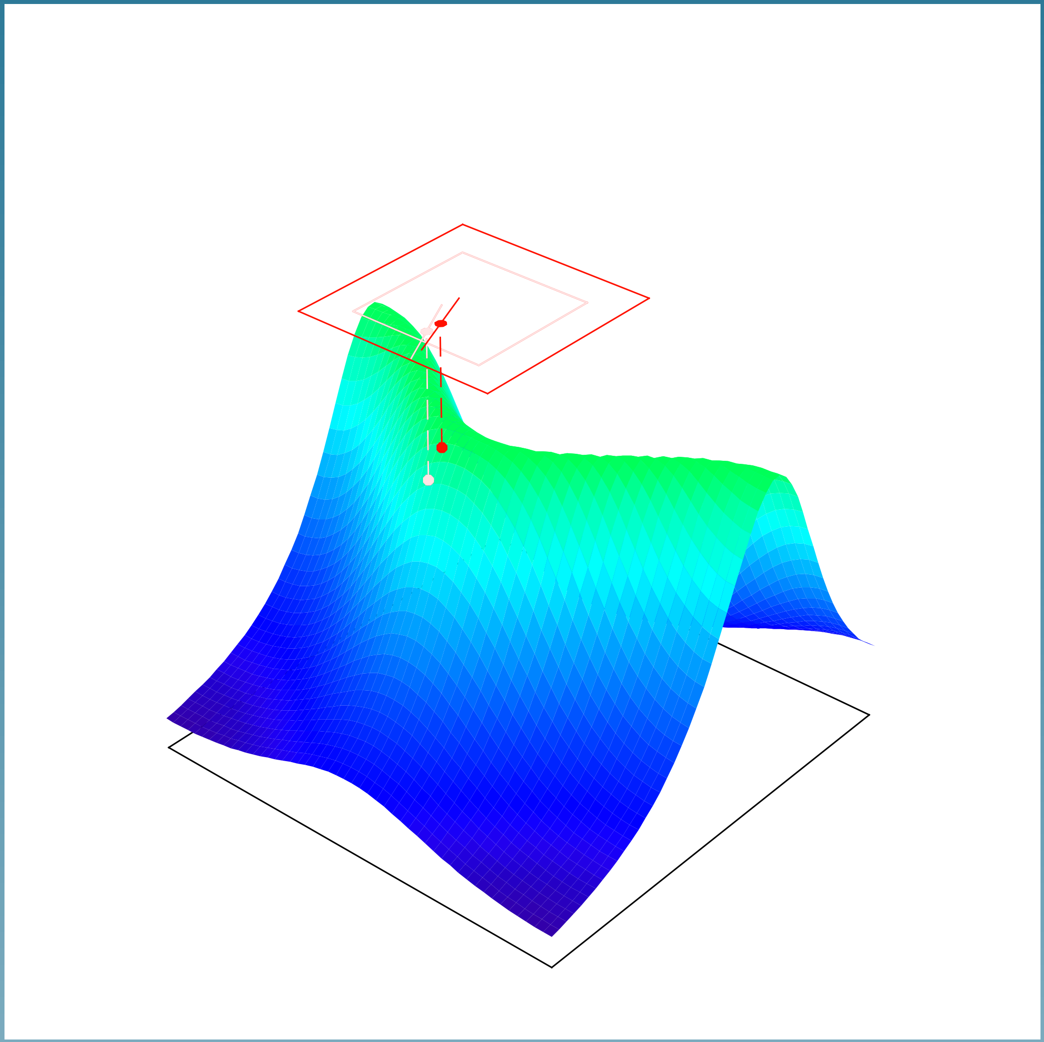

For each window size we obtain an estimate for:

- ridge point location
- ridge orientation angle
- ridge quality

1st step: Ridgel determination via Automated Scaling (Lindeberg, 1993)

For each image pixel we consider multiply sized neighbourhoods:

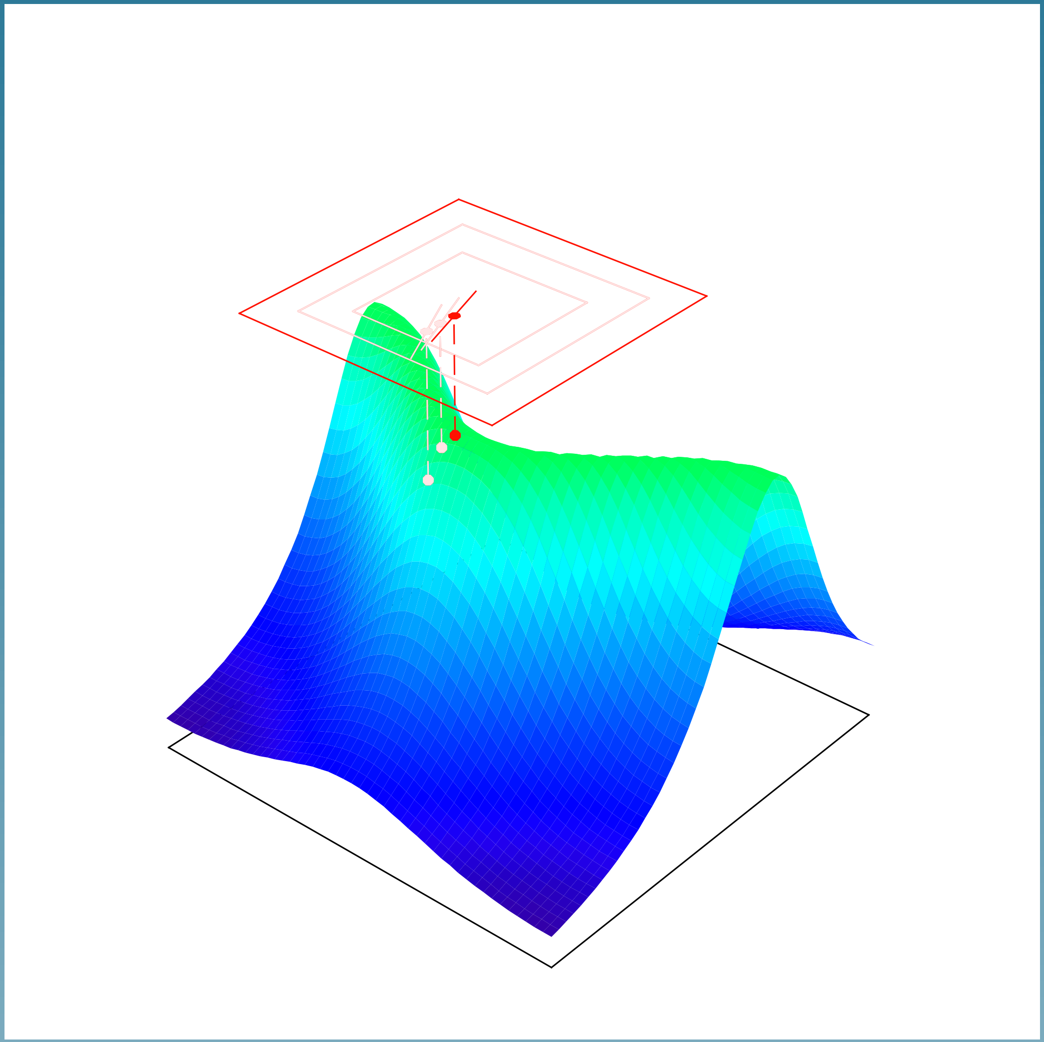

For each window size we obtain an estimate for:

- ridge point location
- ridge orientation angle
- ridge quality

1st step: Ridgel determination via Automated Scaling (Lindeberg, 1993)

For each image pixel we consider multiply sized neighbourhoods:

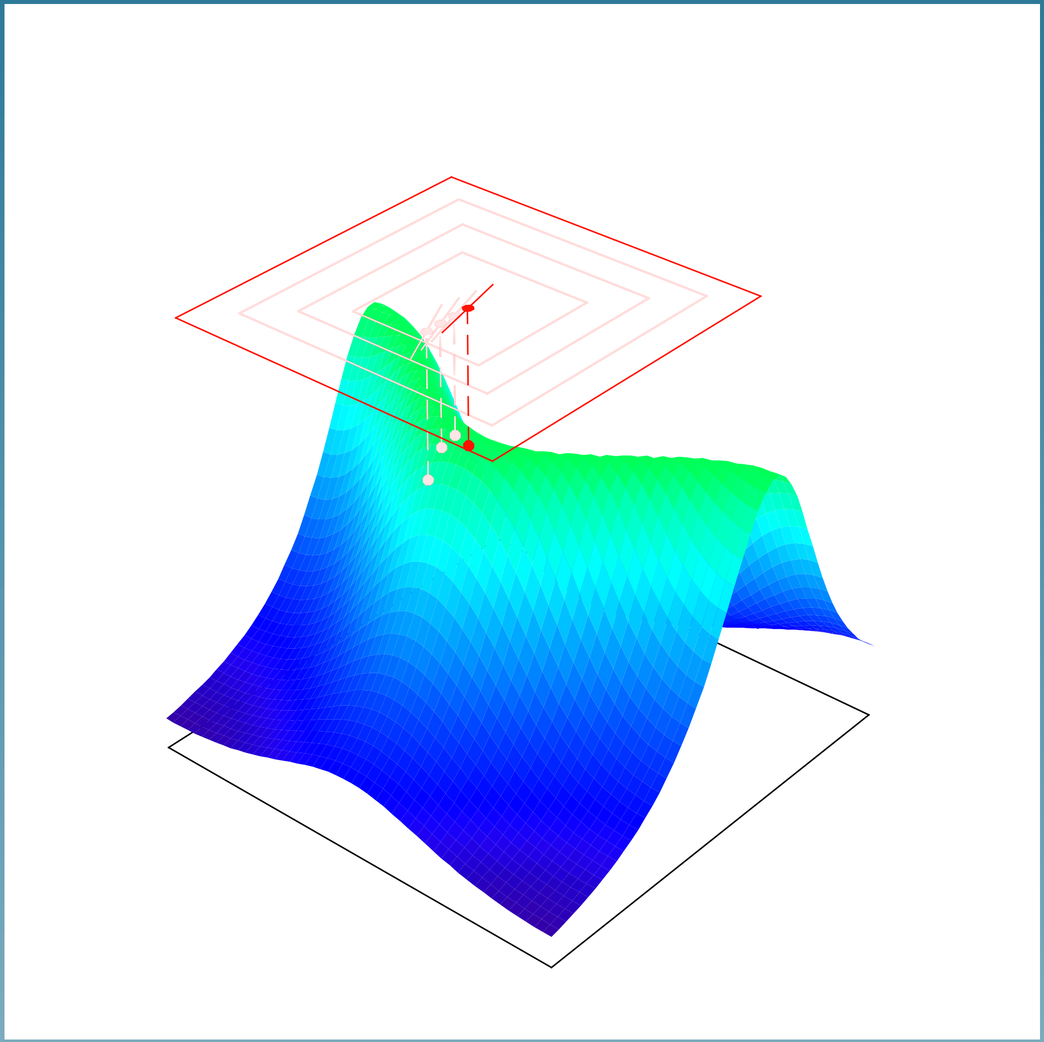

For each window size we obtain an estimate for:

- ridge point location
- ridge orientation angle
- ridge quality

1st step: Ridgel determination via Automated Scaling (Lindeberg, 1993)

For each image pixel we consider multiply sized neighbourhoods:

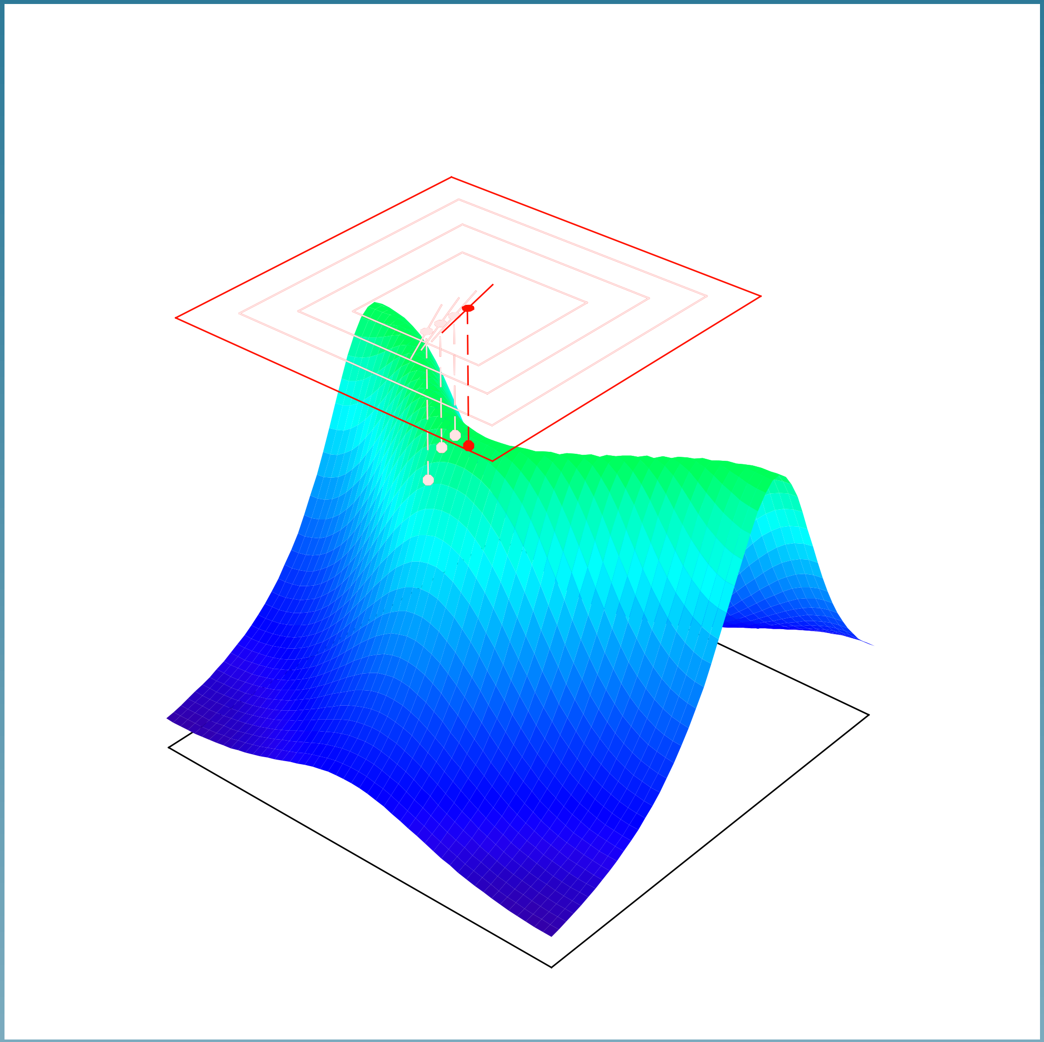

For each window size we obtain an estimate for:

- ridge point location
- ridge orientation angle
- ridge quality

For each pixel the ridge estimate with maximum quality is chosen

2nd step: Ridgel connection via cocircularity measure (Parent and Zucker, 1989)

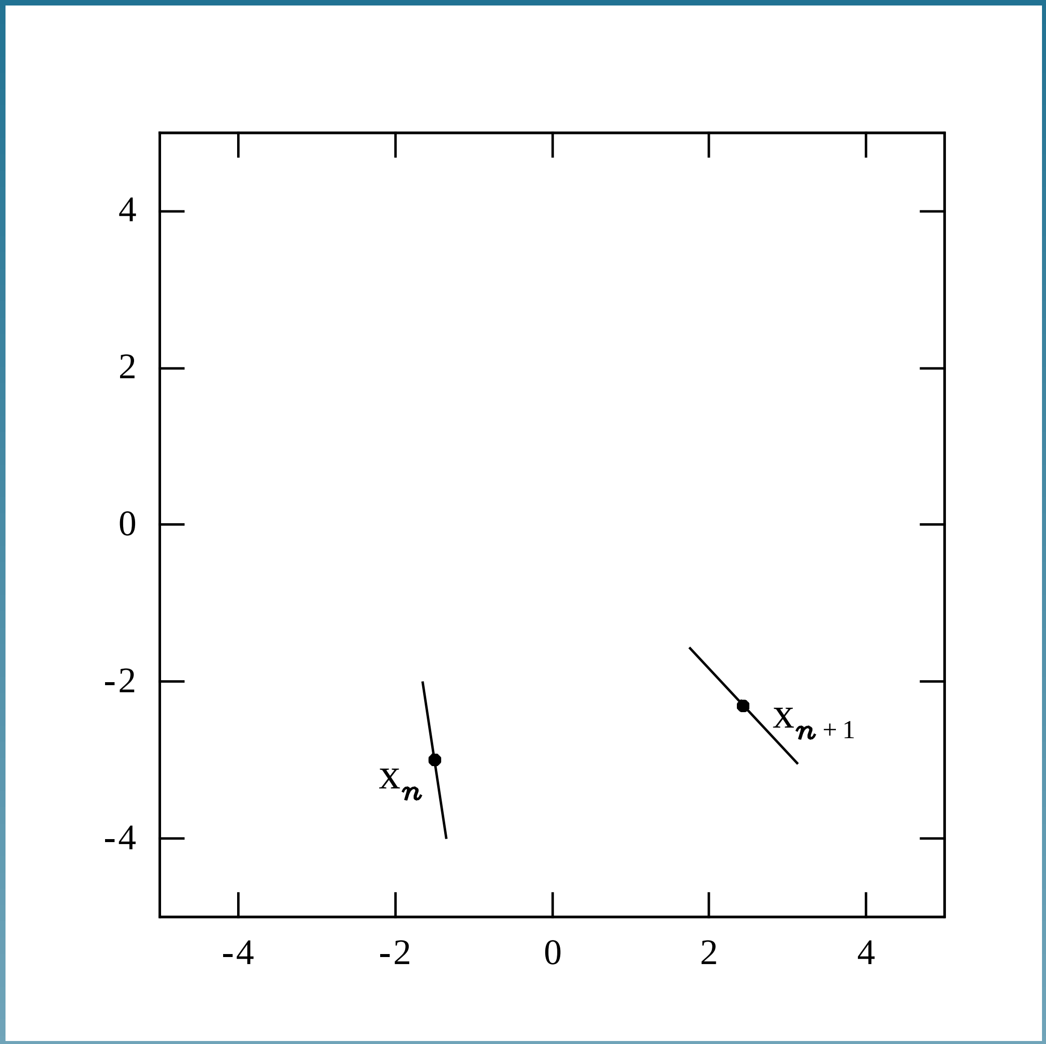

2nd step: Ridgel connection via cocircularity measure (Parent and Zucker, 1989)

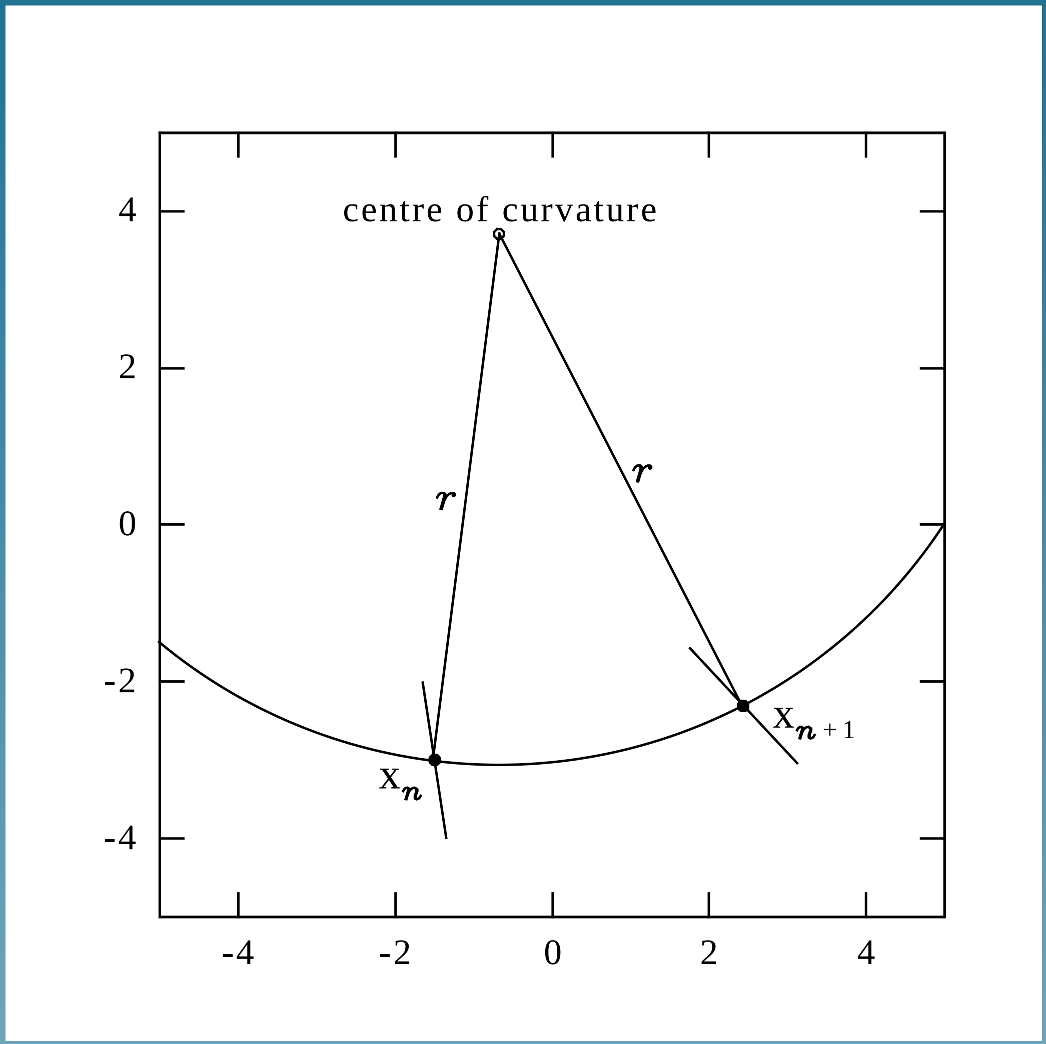

2nd step: Ridgel connection via cocircularity measure (Parent and Zucker, 1989)

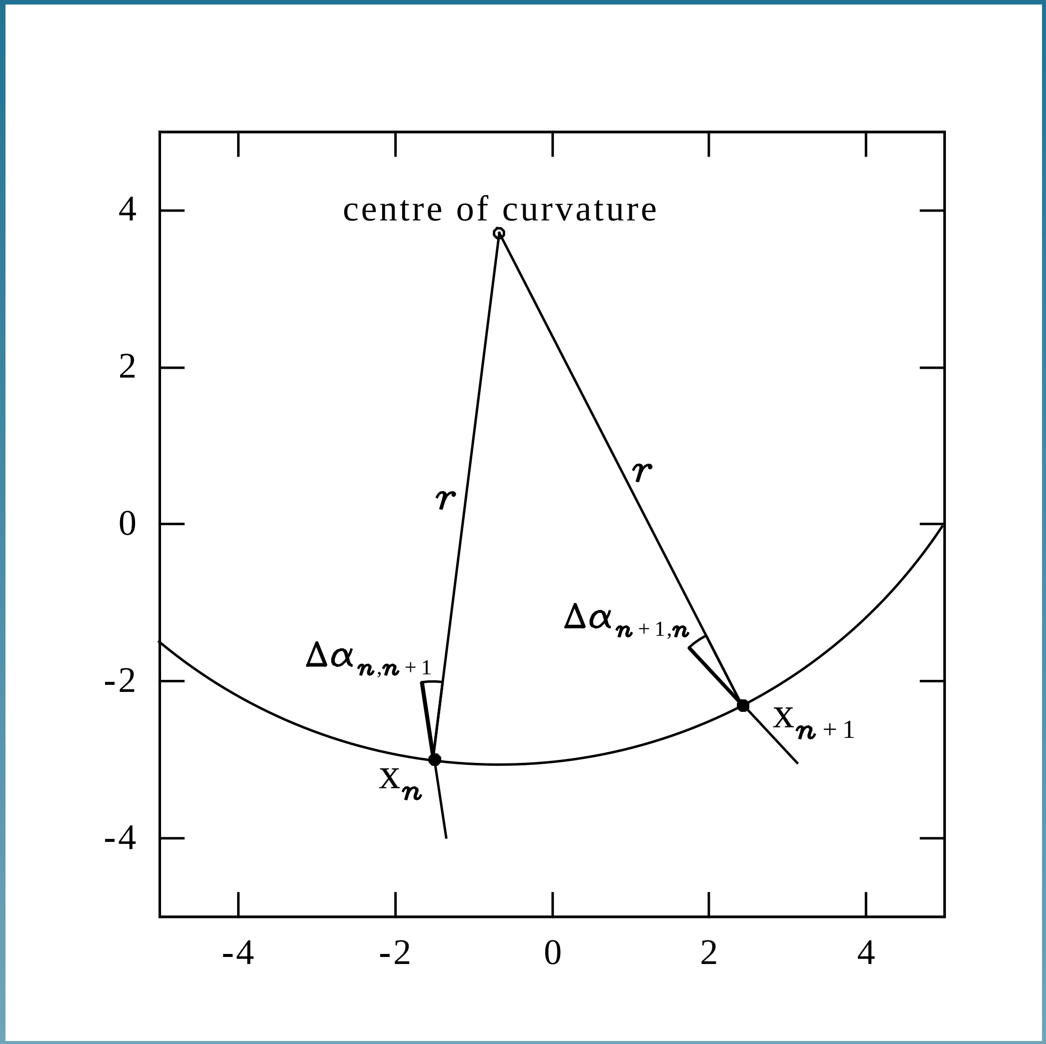

2nd step: Ridgel connection via cocircularity measure (Parent and Zucker, 1989)

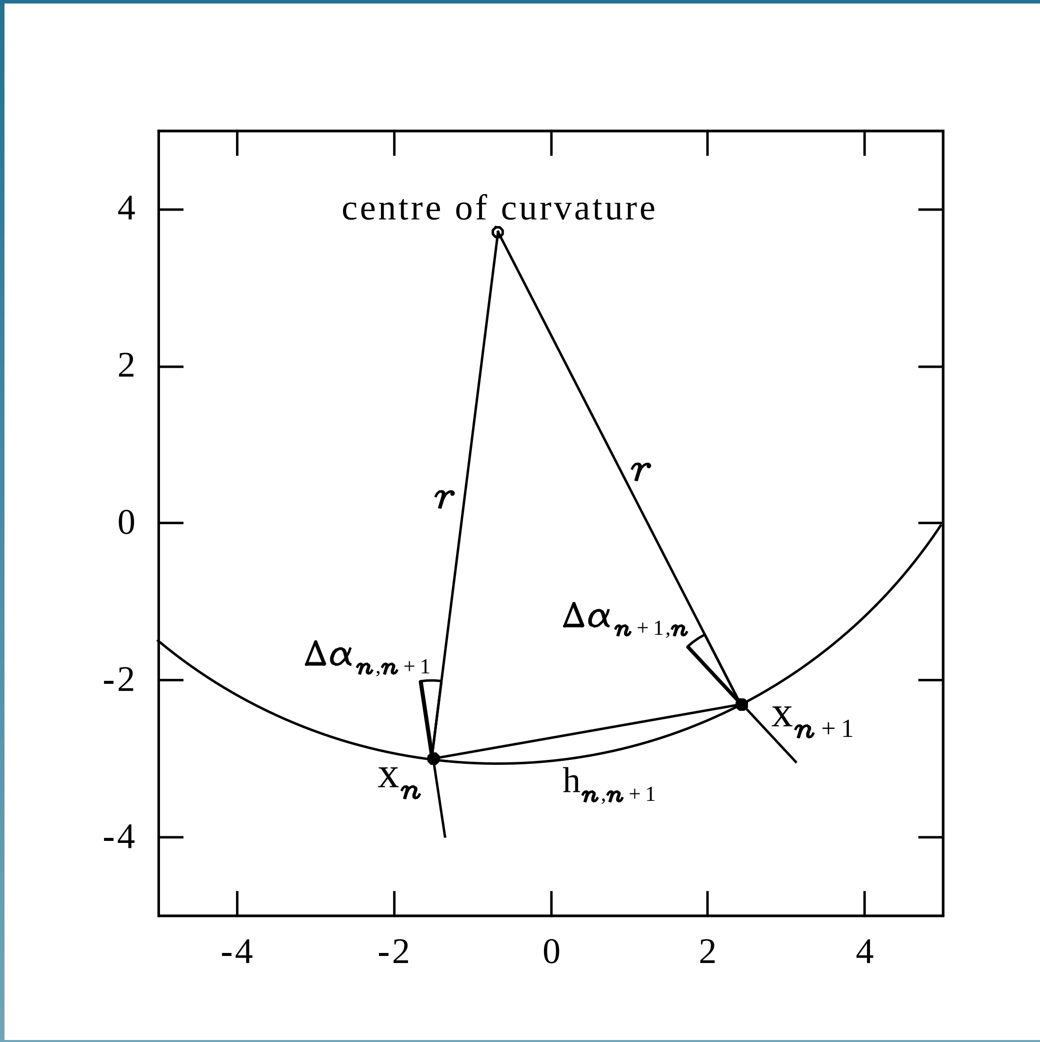

2nd step: Ridgel connection via cocircularity measure (Parent and Zucker, 1989)

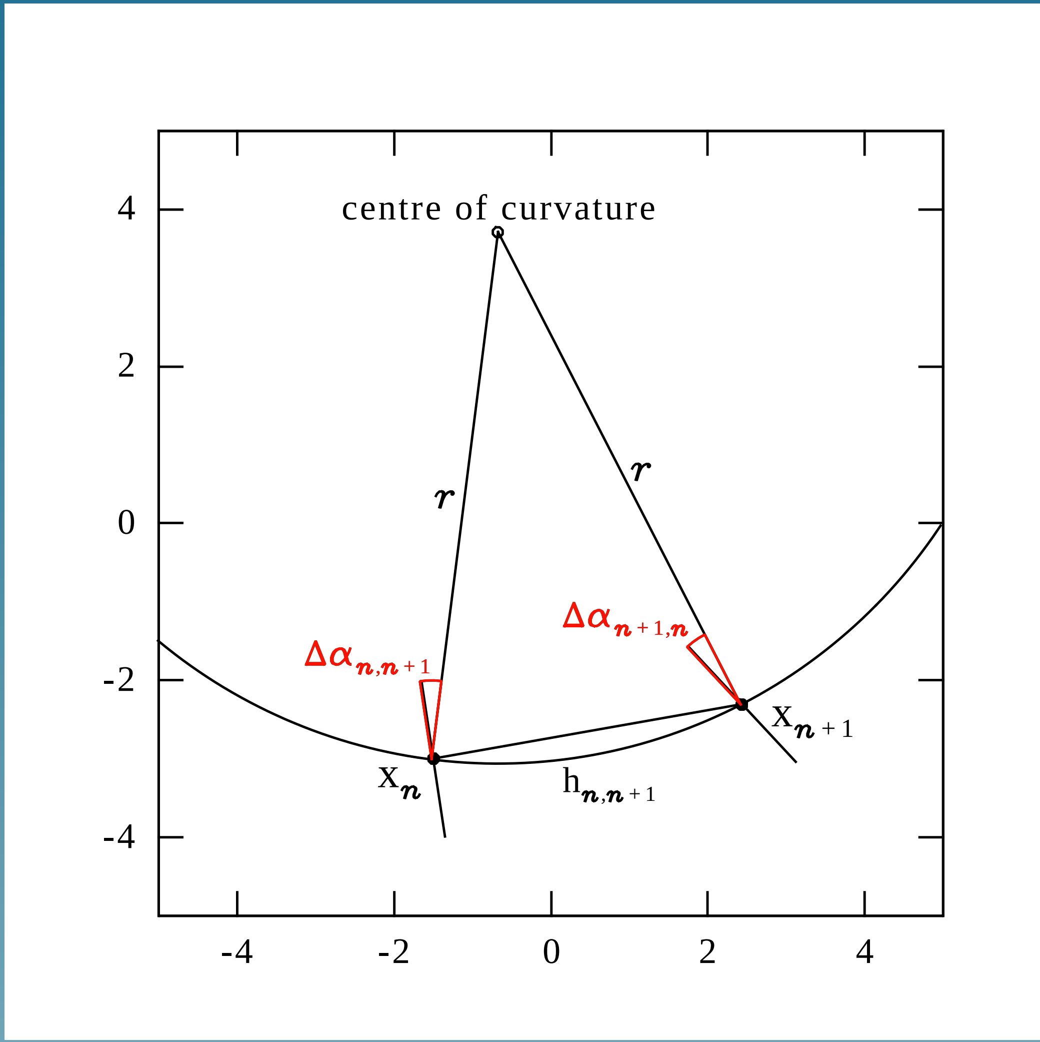

The selected connections minimize the sum of:

$$\frac{\Delta\alpha^2_{n,n+1}}{\alpha^2_{\text{scal}}}$$

2nd step: Ridgel connection via cocircularity measure (Parent and Zucker, 1989)

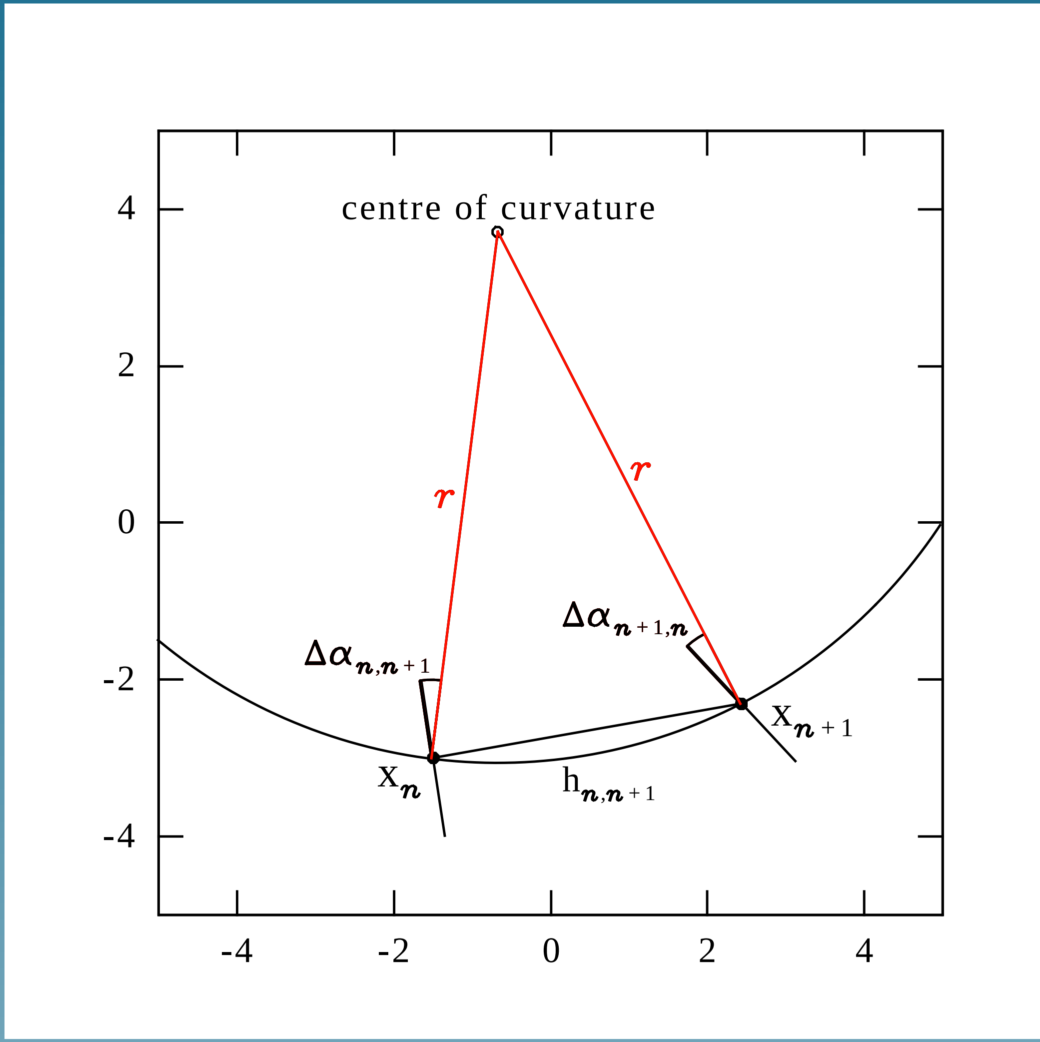

The selected connections minimize the sum of:

$$\frac{\Delta\alpha_{n,n+1}^2}{\alpha_{\mathrm{scal}}^2} + \frac{r_{\mathrm{scal}}^2}{r^2}$$

2nd step: Ridgel connection via cocircularity measure (Parent and Zucker, 1989)

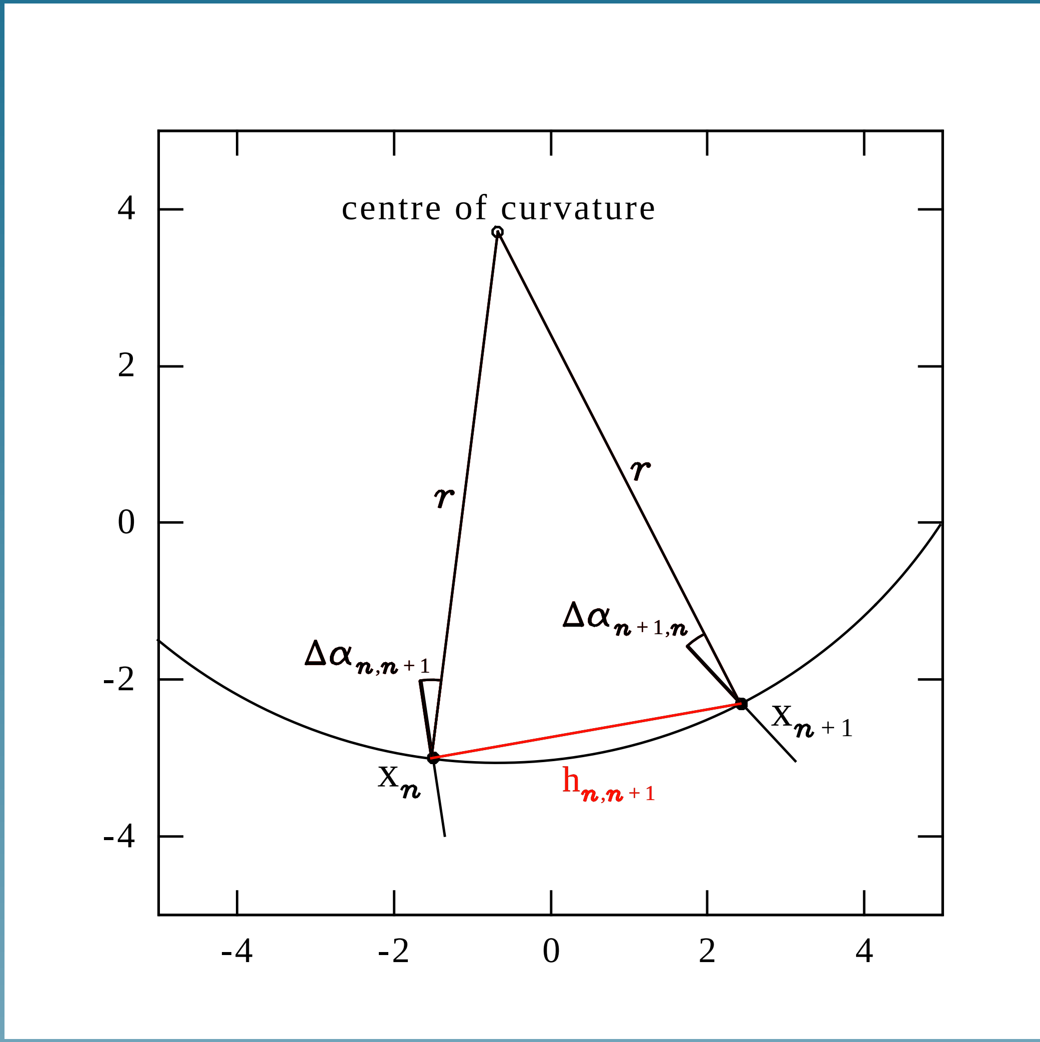

The selected connections minimize the sum of:

$$\frac{\Delta\alpha^2_{n,n+1}}{\alpha^2_{\mathrm{scal}}} + \frac{r^2_{\mathrm{scal}}}{r^2} + \frac{h^2_{n,n+1}}{h^2_{\mathrm{scal}}}$$

2nd step: Ridgel connection via cocircularity measure (Parent and Zucker, 1989)

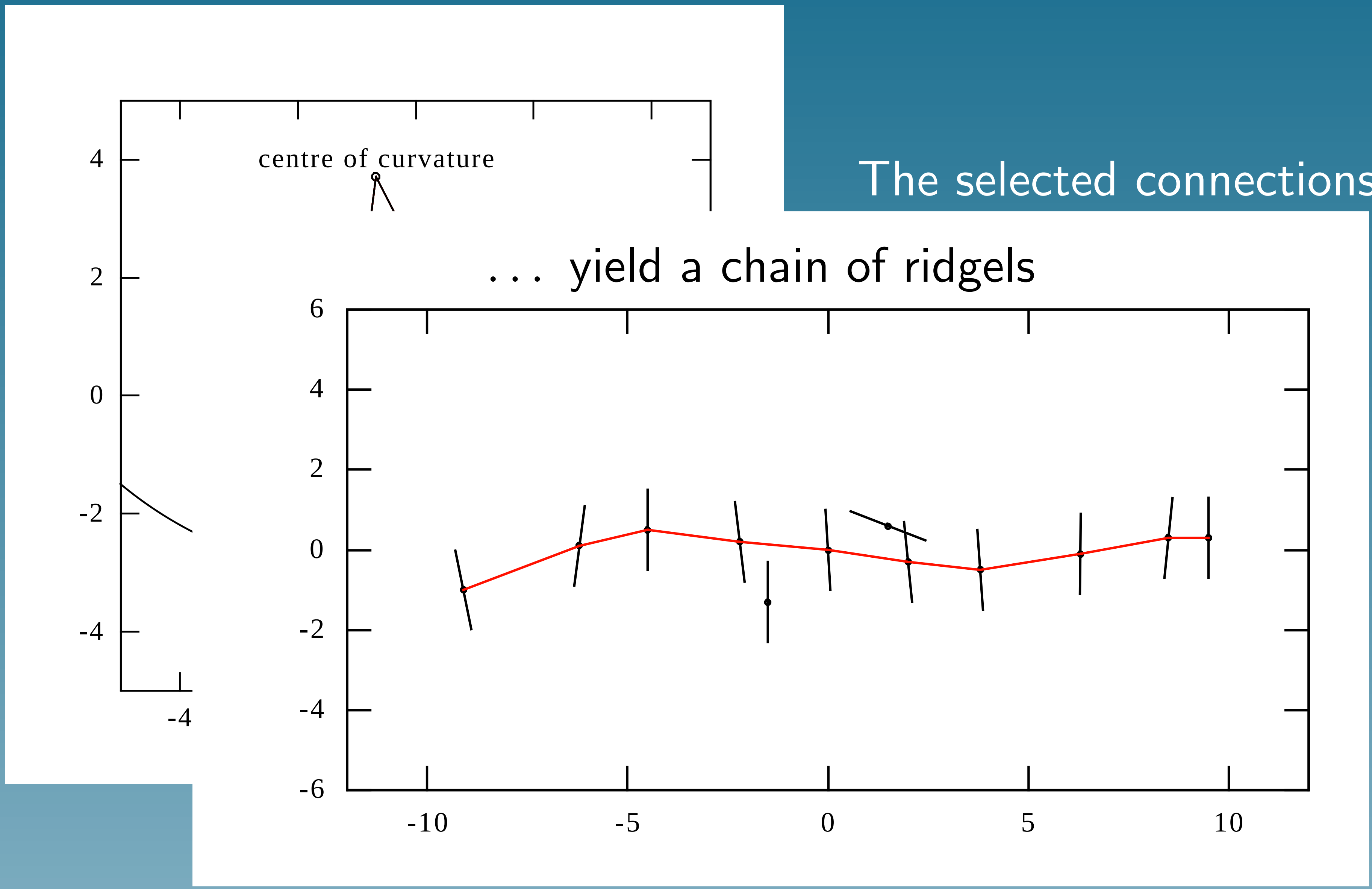

3rd step: Chain fit by parametric smoothing splines

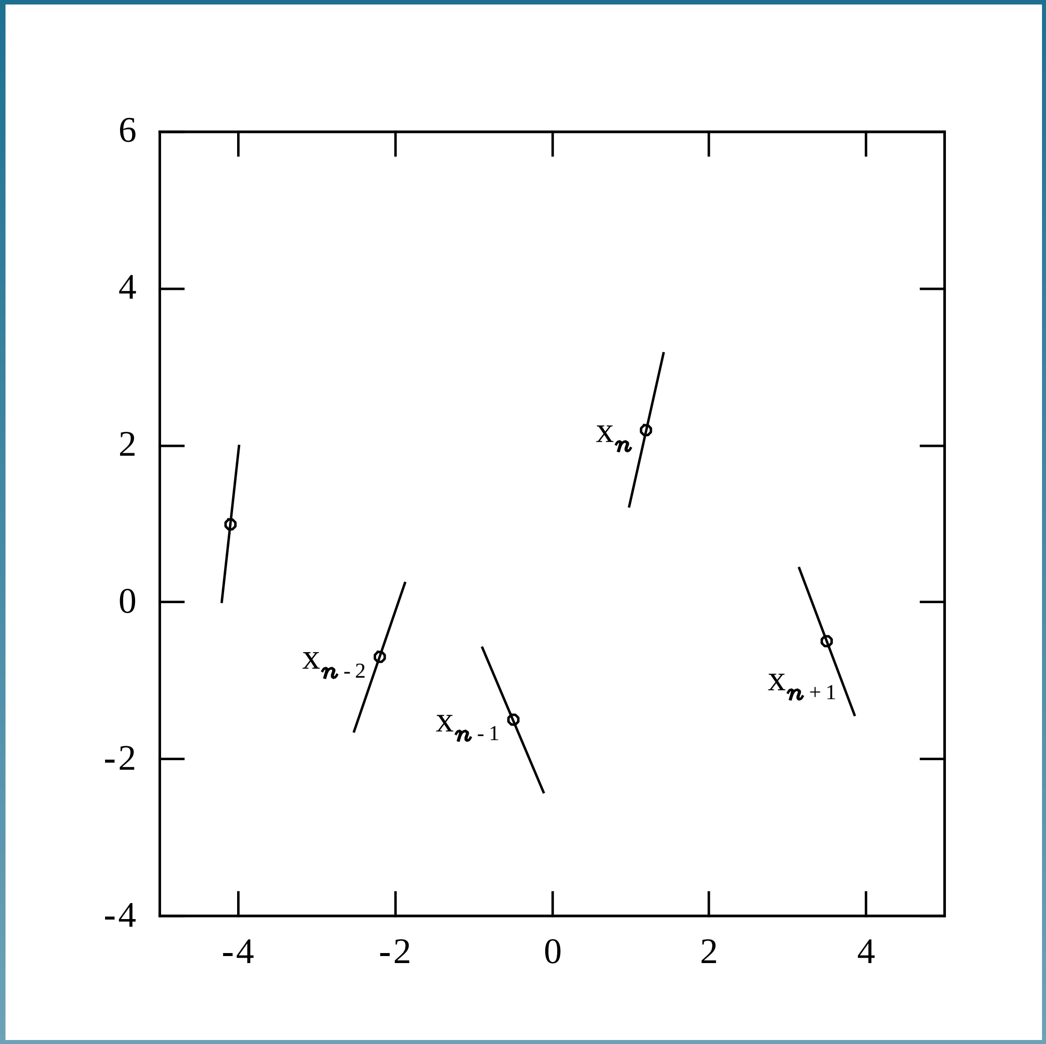

3rd step: Chain fit by parametric smoothing splines

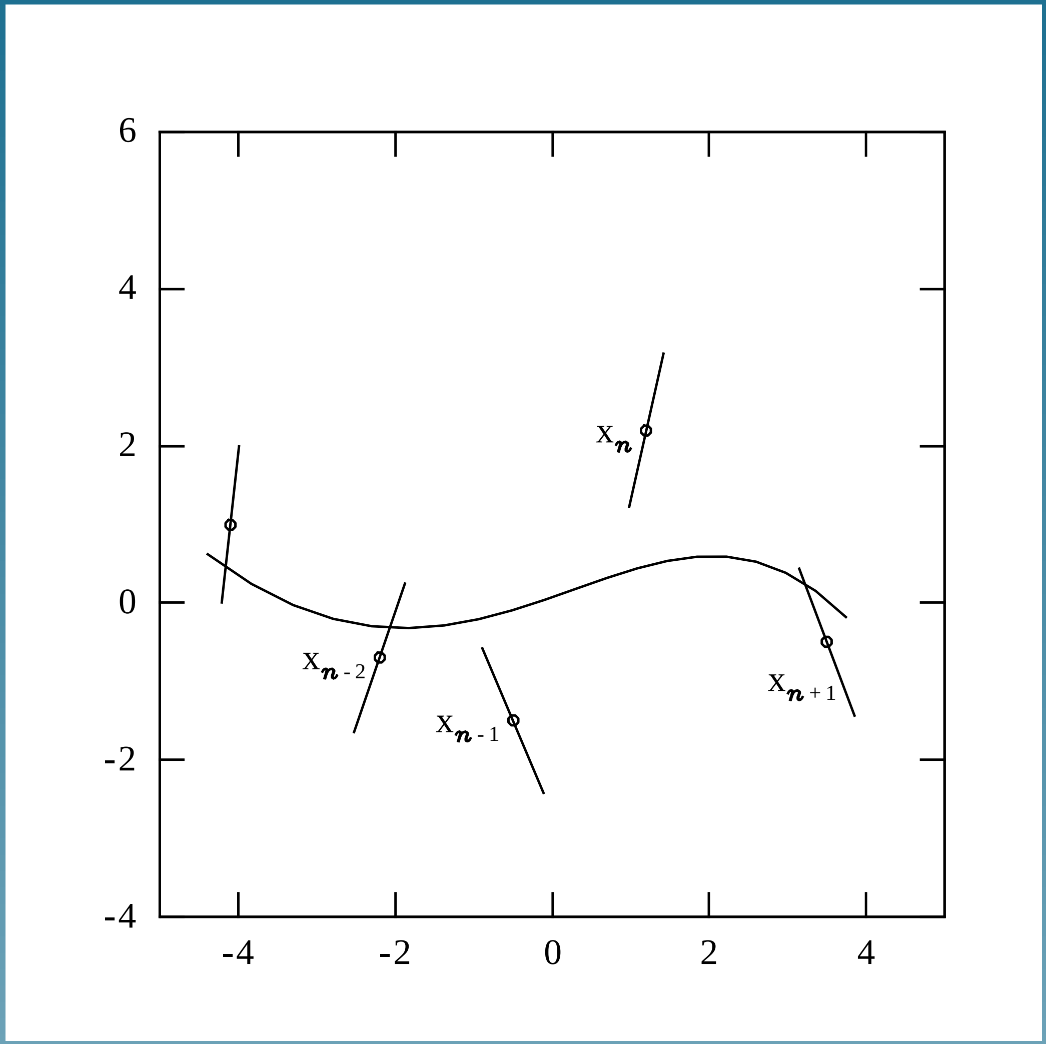

The smoothing spline is constrained by the minimization of:

3rd step: Chain fit by parametric smoothing splines

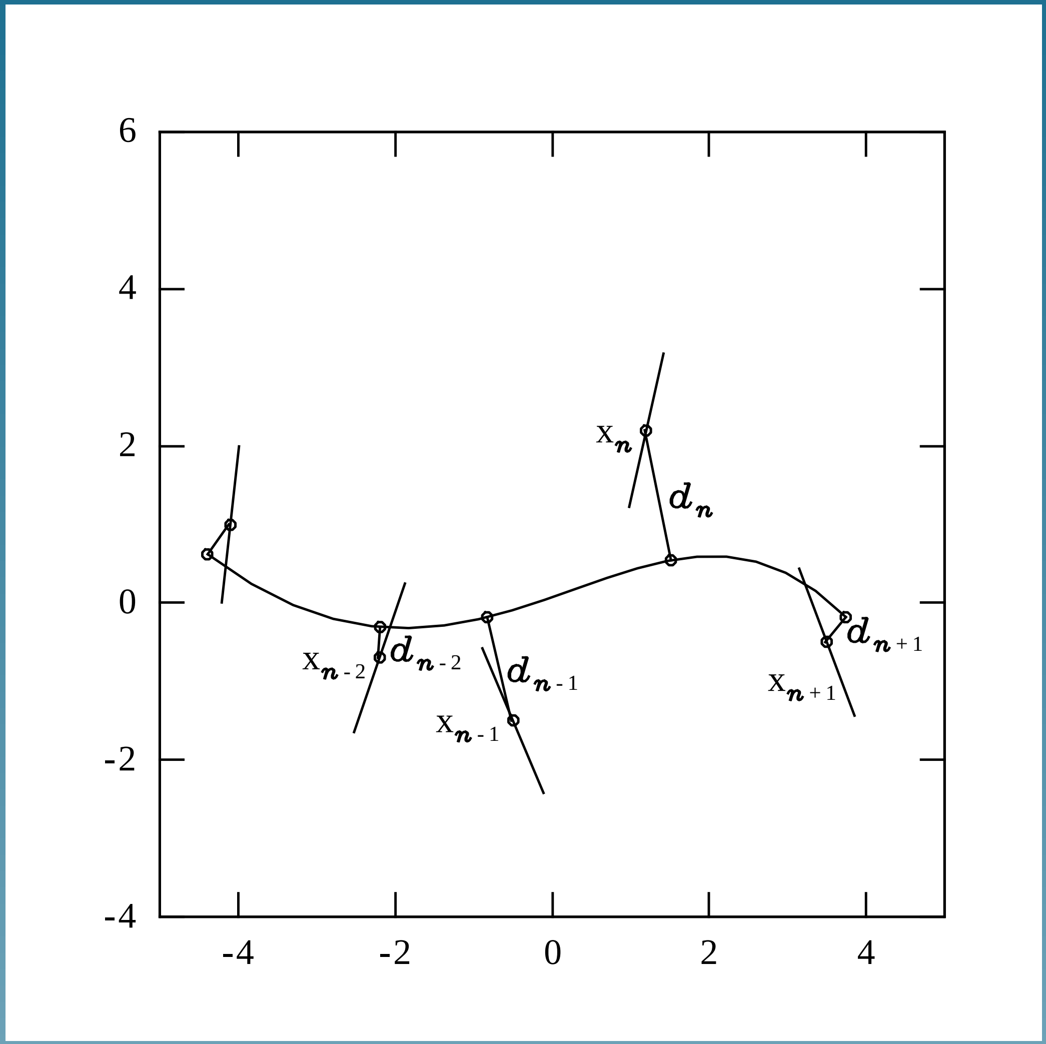

The smoothing spline is constrained by the minimization of:

$$\sum_{i \in \text{chain}} \frac{d_i^2}{d_{\text{scal}}^2}$$

3rd step: Chain fit by parametric smoothing splines

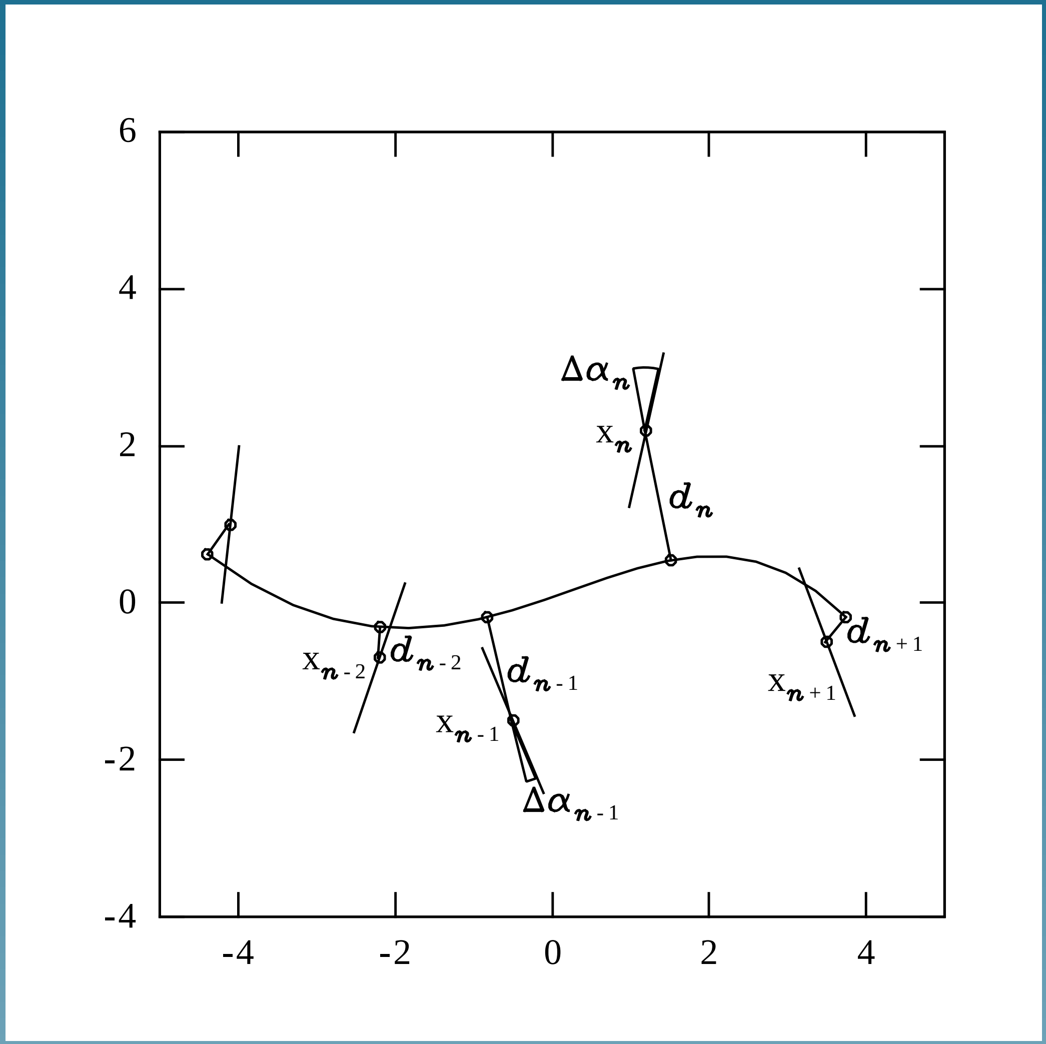

The smoothing spline is constrained by the minimization of:

$$\sum_{i\in\text{chain}} \frac{d_i^2}{d_{\text{scal}}^2}$$
$$\sum_{i\in\text{chain}} + \frac{\Delta\alpha_i^2}{\alpha_{\text{scal}}^2}$$

3rd step: Chain fit by parametric smoothing splines

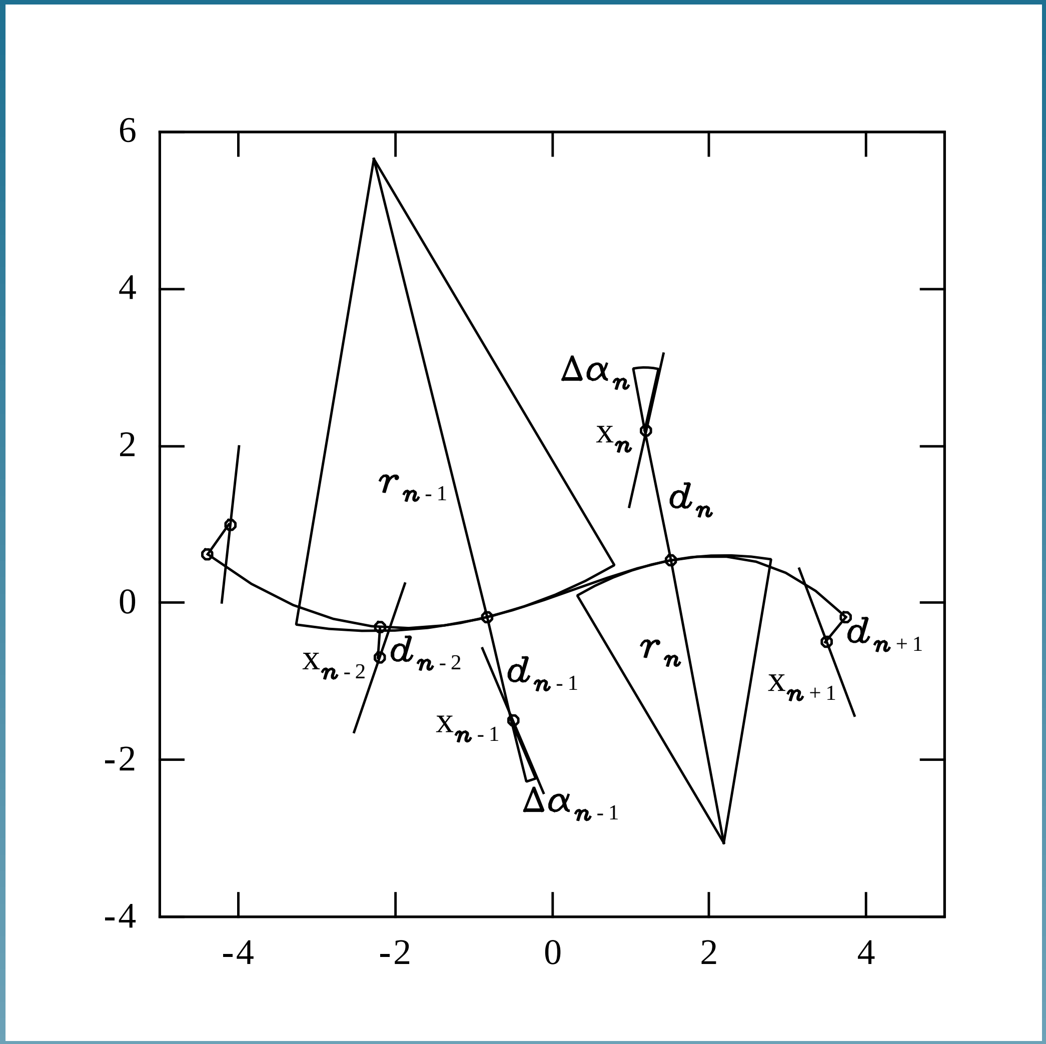

The smoothing spline is constrained by the minimization of:

$$\sum_{i\in\text{chain}} \frac{d_i^2}{d_{\text{scal}}^2} + \sum_{i\in\text{chain}} \frac{\Delta\alpha_i^2}{\alpha_{\text{scal}}^2} + \int_{\text{fit curve}} \frac{r_{\text{scal}}^2}{r^2(s)}\, ds$$

3rd step: Chain fit by parametric smoothing splines

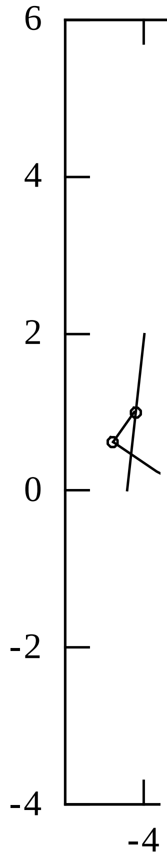

The smoothing spline

. . . yields an approximation to a loop segment

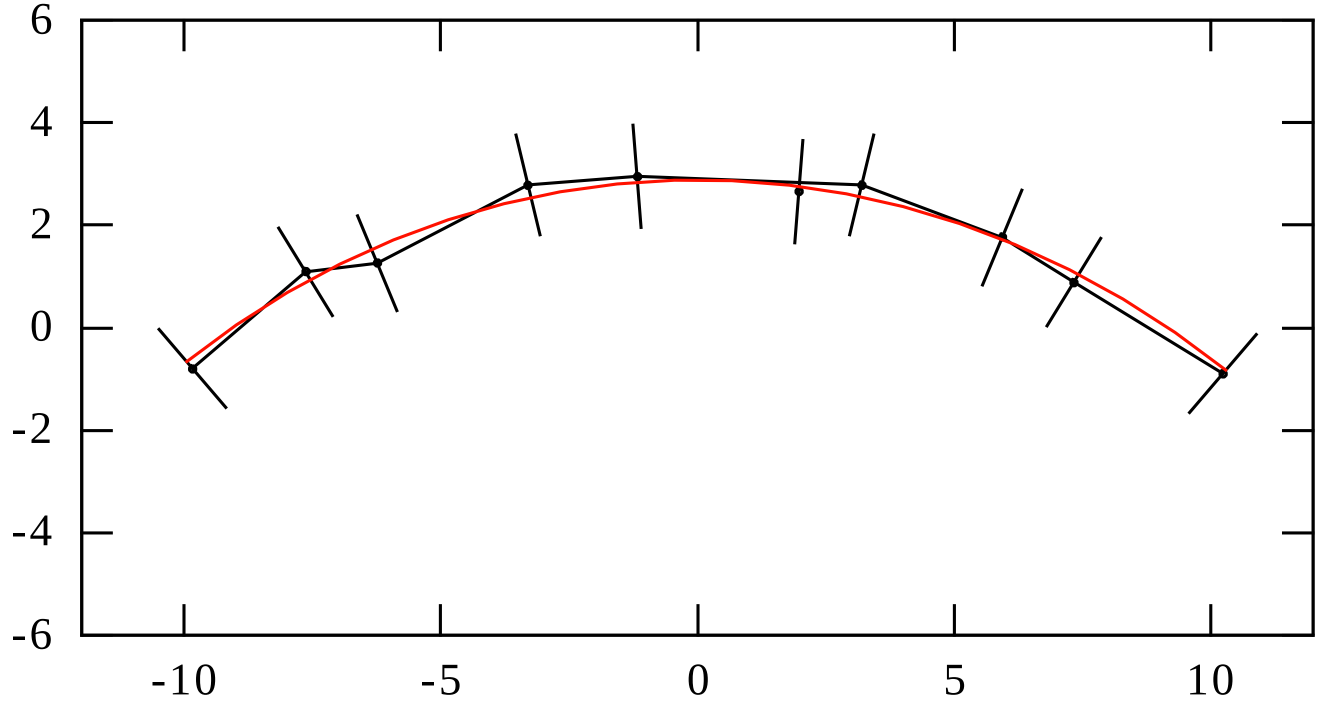

4th step: Interactive postpolishing

No program is perfect. . .

4th step: Interactive postpolishing

No program is perfect. . .
we therefore provide the possibility to modify the results:

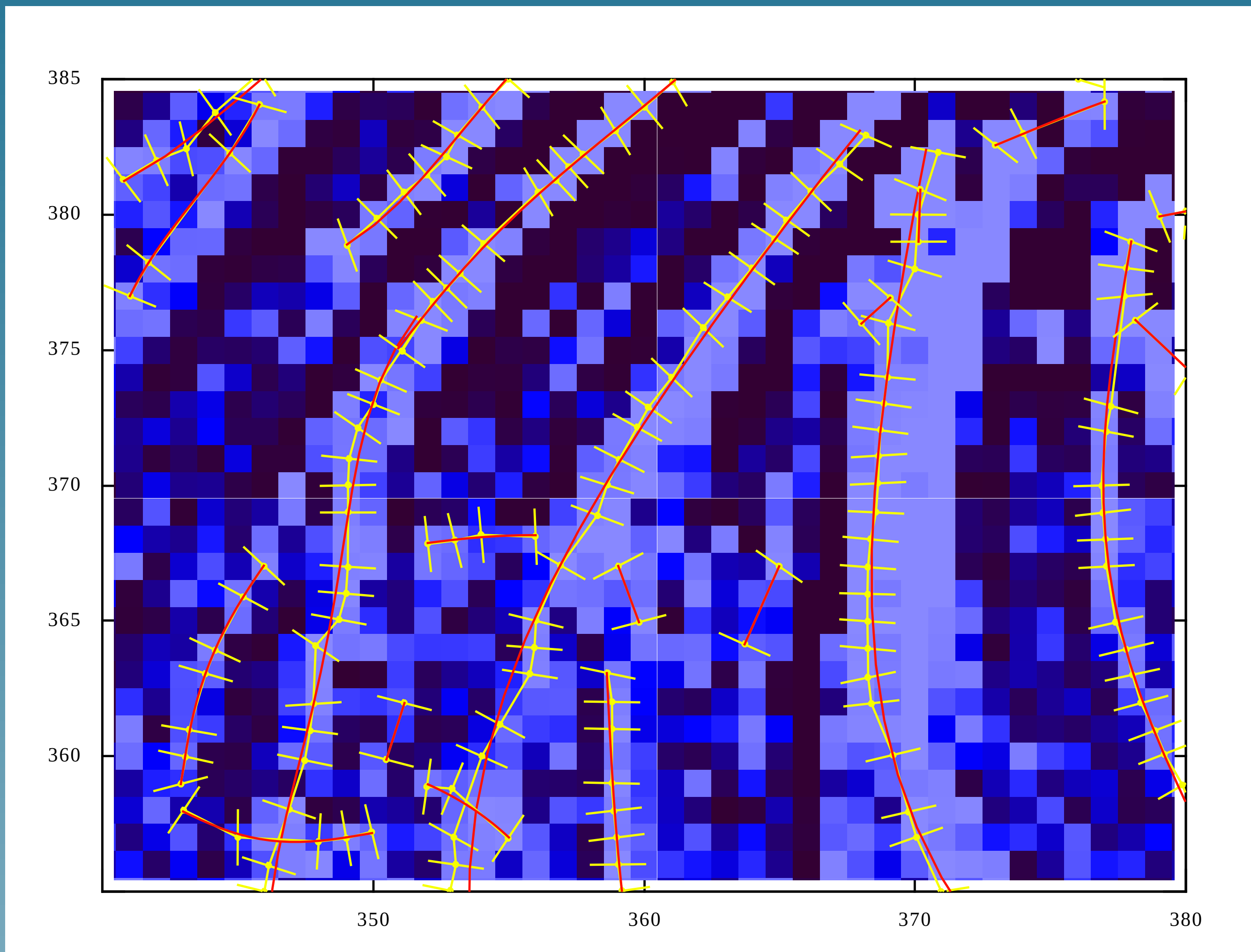

4th step: Interactive postpolishing

No program is perfect. . .
we therefore provide the possibility to modify the results:

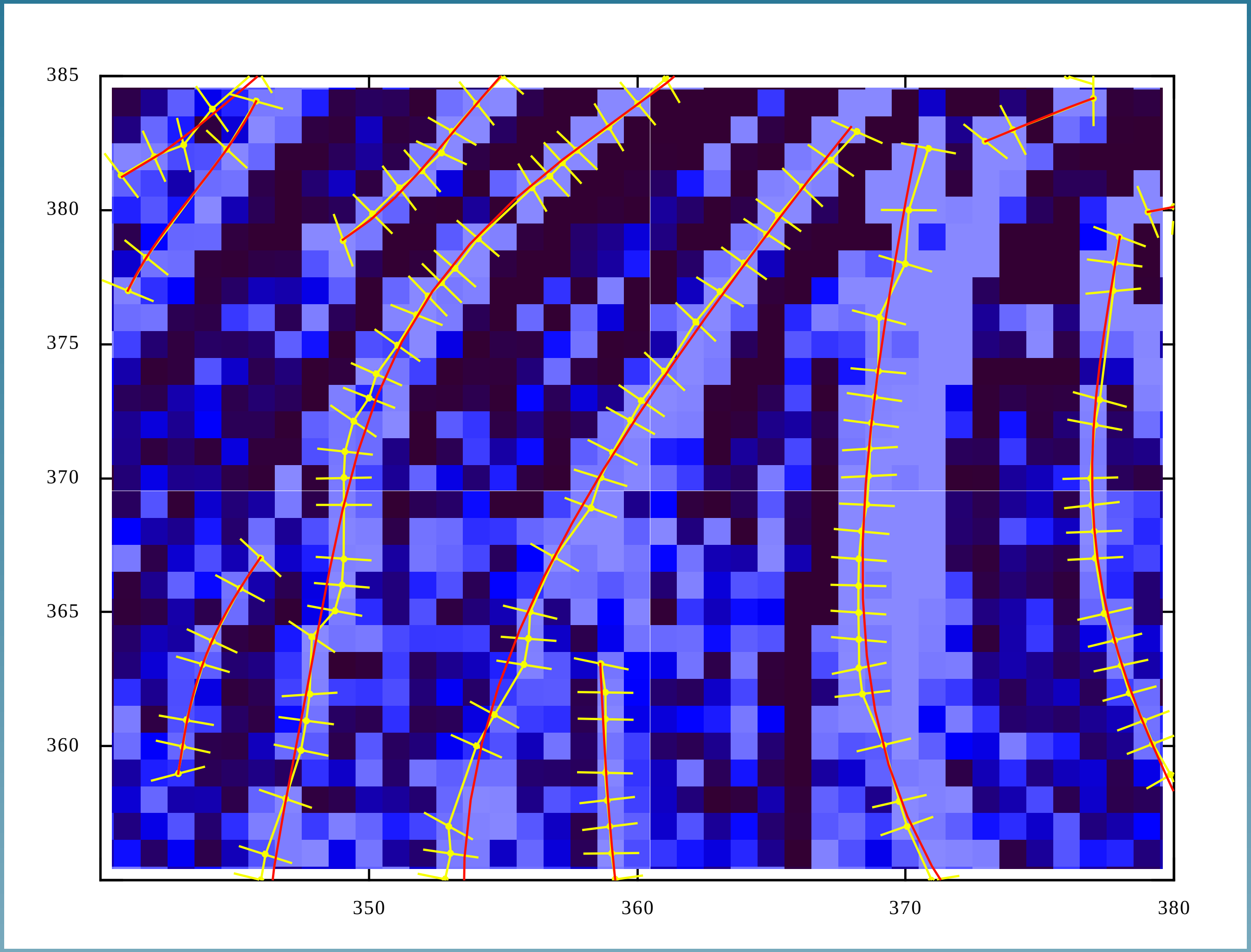

- eliminate unwanted curves

4th step: Interactive postpolishing

No program is perfect. . .
we therefore provide the possibility to modify the results:

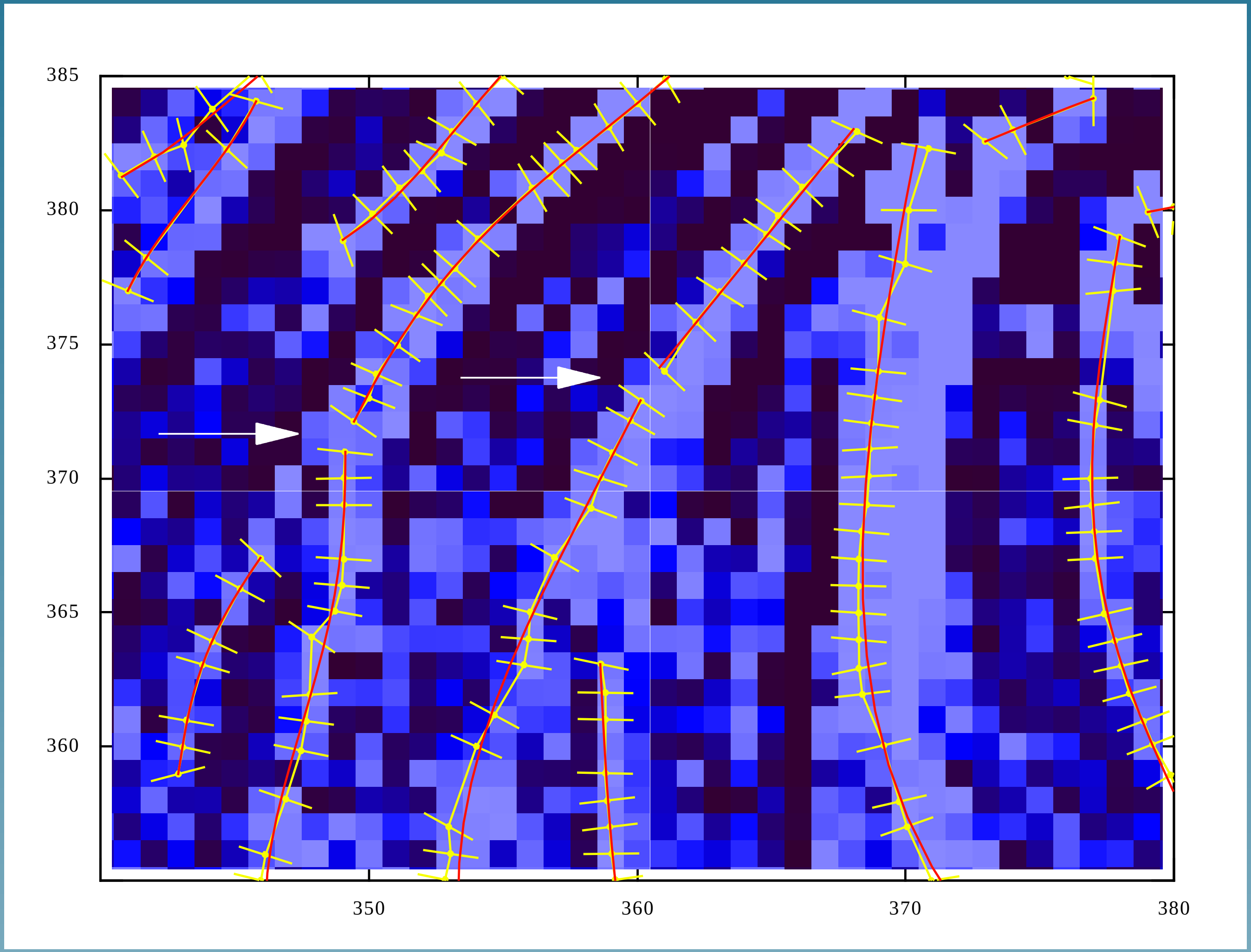

- eliminate unwanted curves
- split curves

4th step: Interactive postpolishing

No program is perfect. . .
we therefore provide the possibility to modify the results:

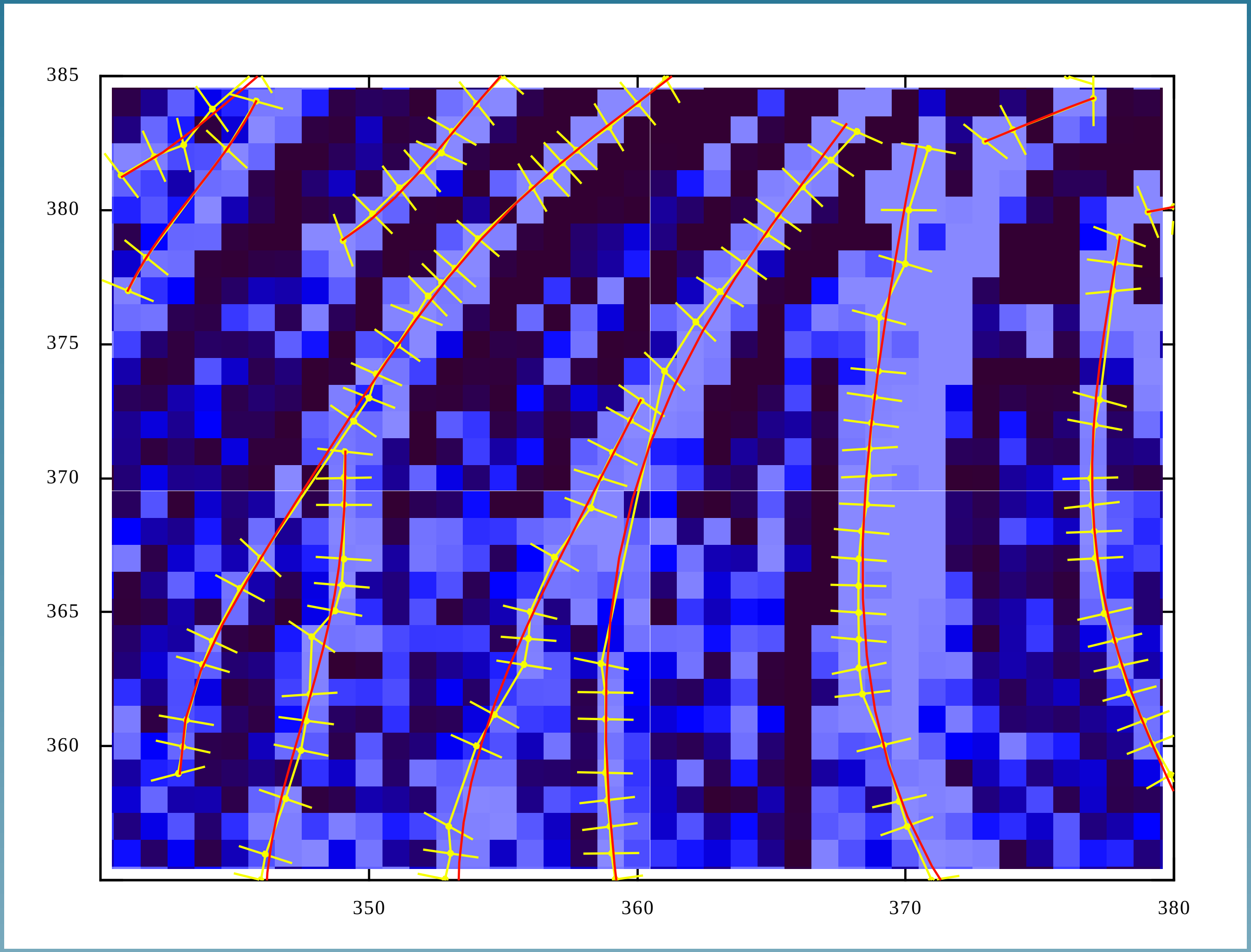

- eliminate unwanted curves
- split curves
- merge curves

Application to SECCHI EUVI images

Original image: an active region from 2006-12-12

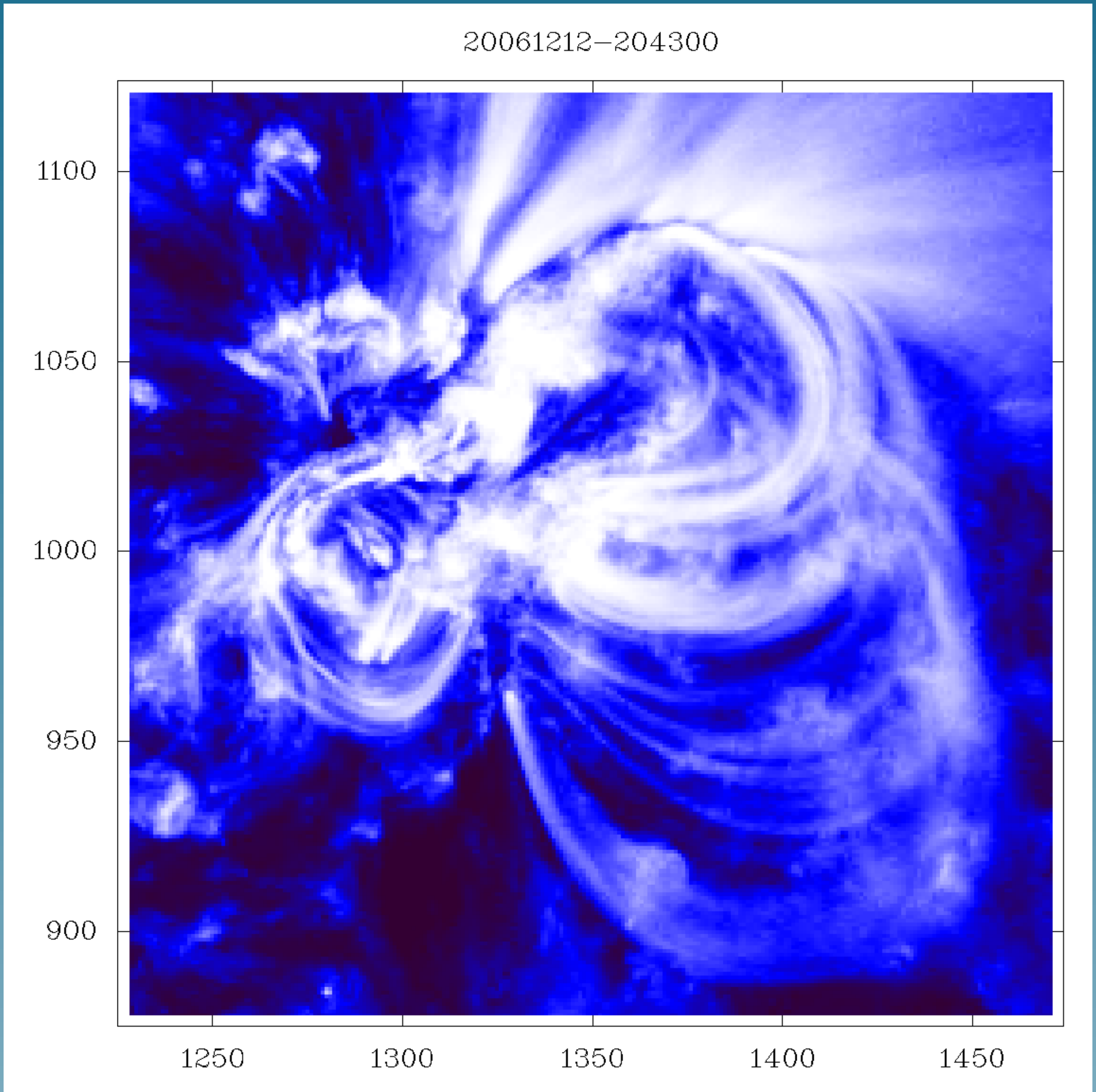

Application to SECCHI EUVI images

Quality coefficient: derived from the eigenvalues of $\boldsymbol{H}$

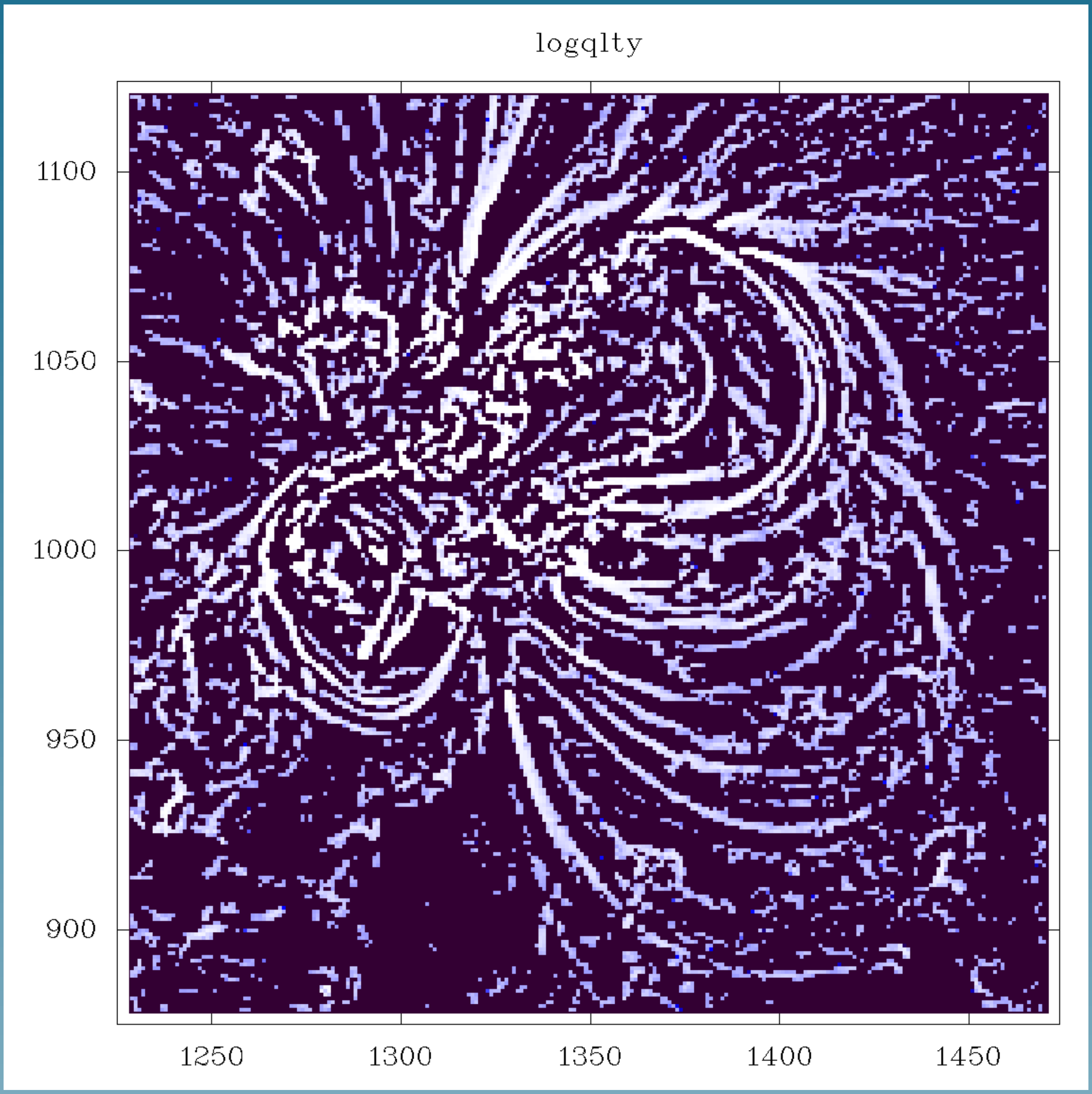

Application to SECCHI EUVI images

Quality coefficient: derived from the eigenvalues of $\boldsymbol{H}$

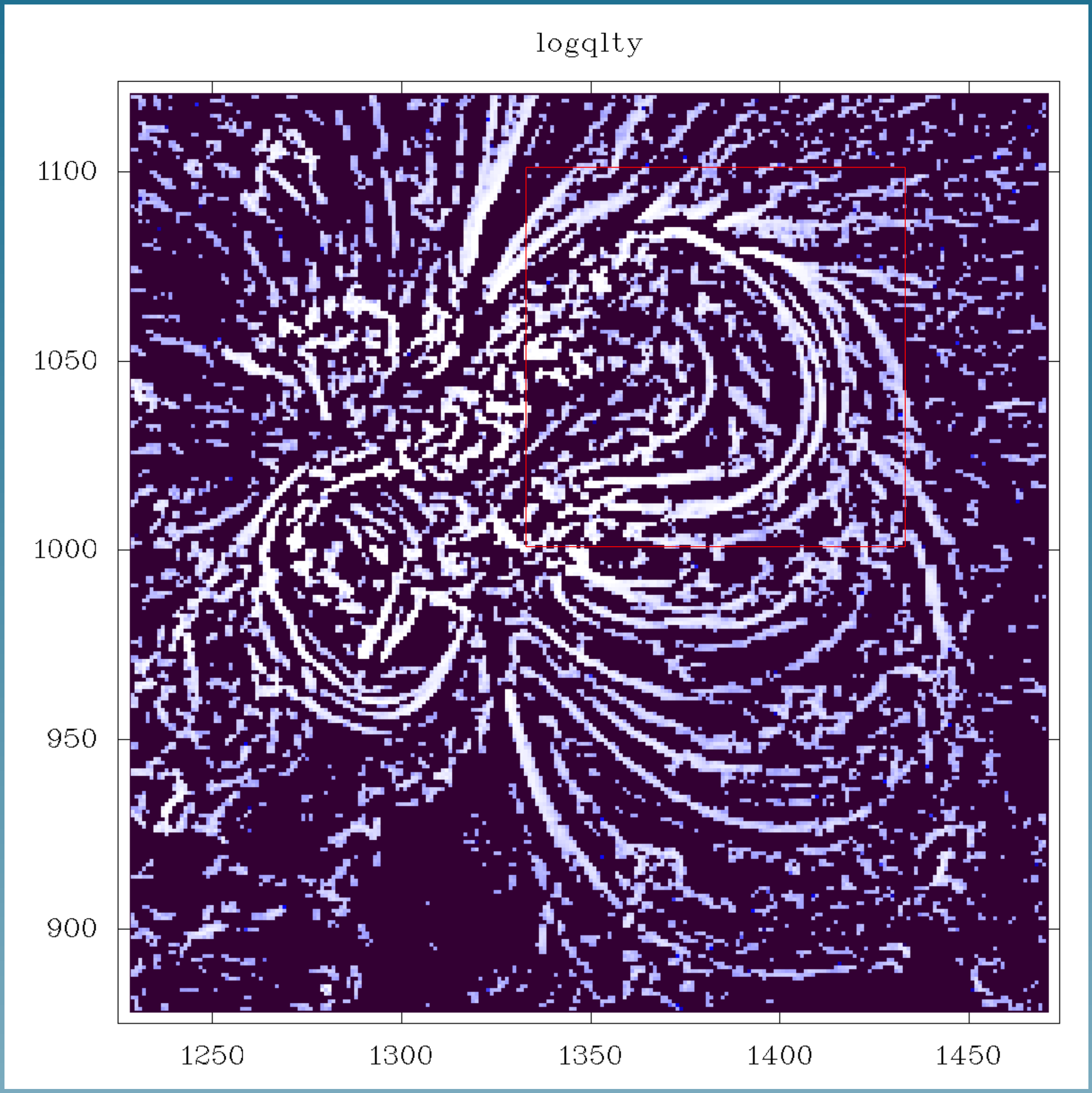

Application to SECCHI EUVI images

Ridgel orientation: derived from the eigenvectors $\boldsymbol{e}_i$ of $\boldsymbol{H}$

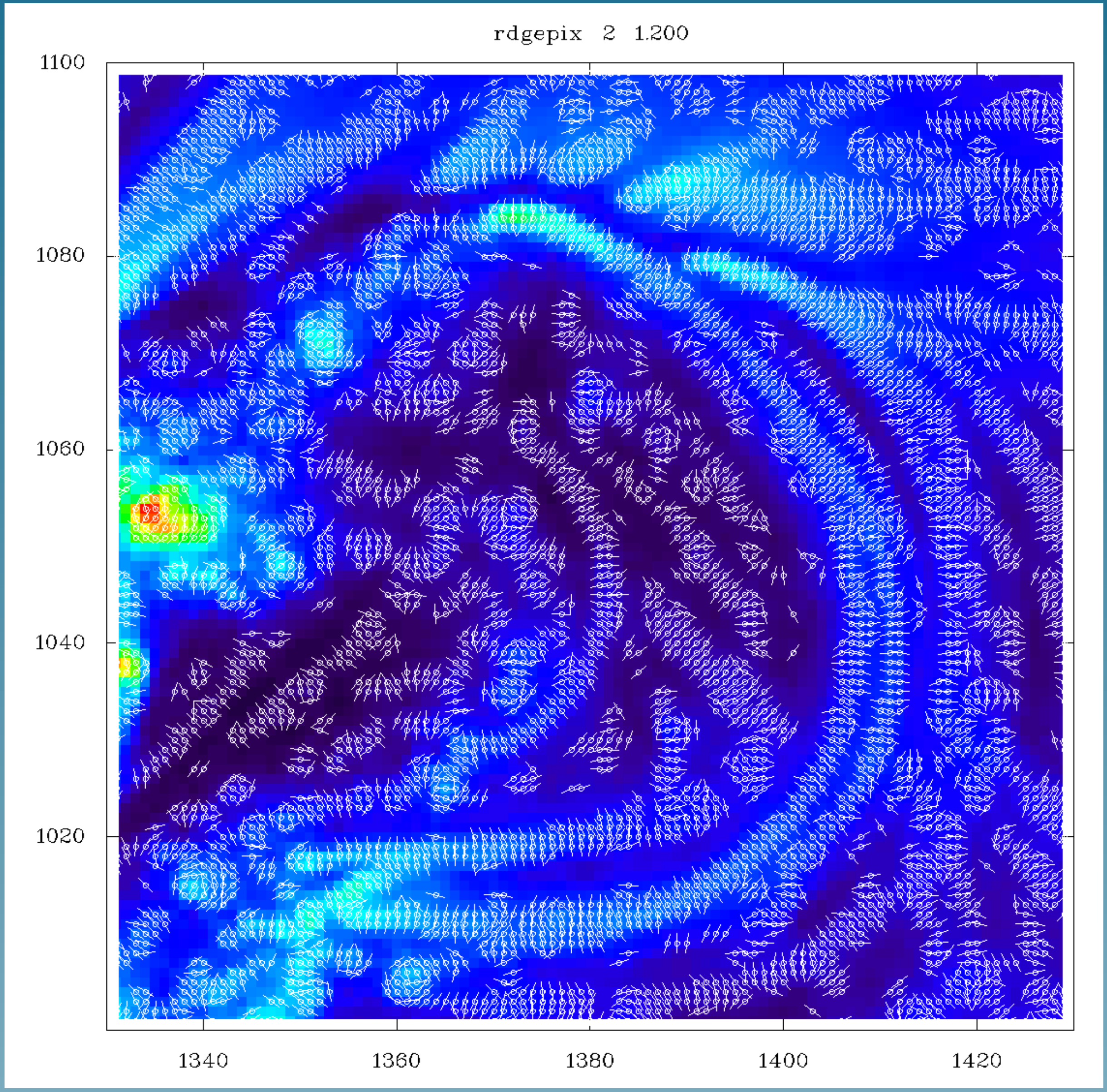

Application to SECCHI EUVI images

Ridgel position: interpolated from the sign change of $(\boldsymbol{g}^T \boldsymbol{e}_1)$

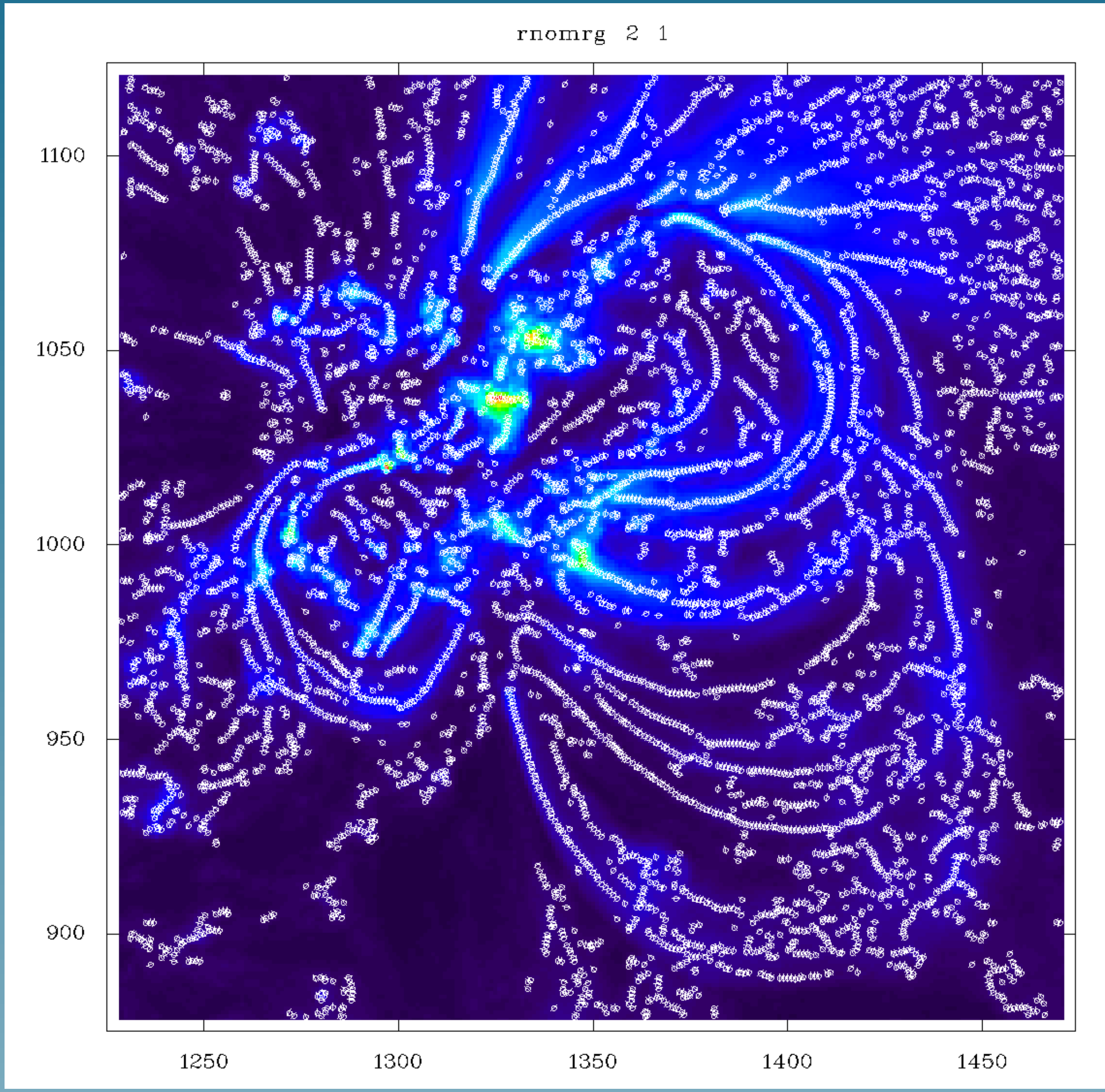

Application to SECCHI EUVI images

Ridgel position: interpolated from the sign change of $(\boldsymbol{g}^T \boldsymbol{e}_1)$

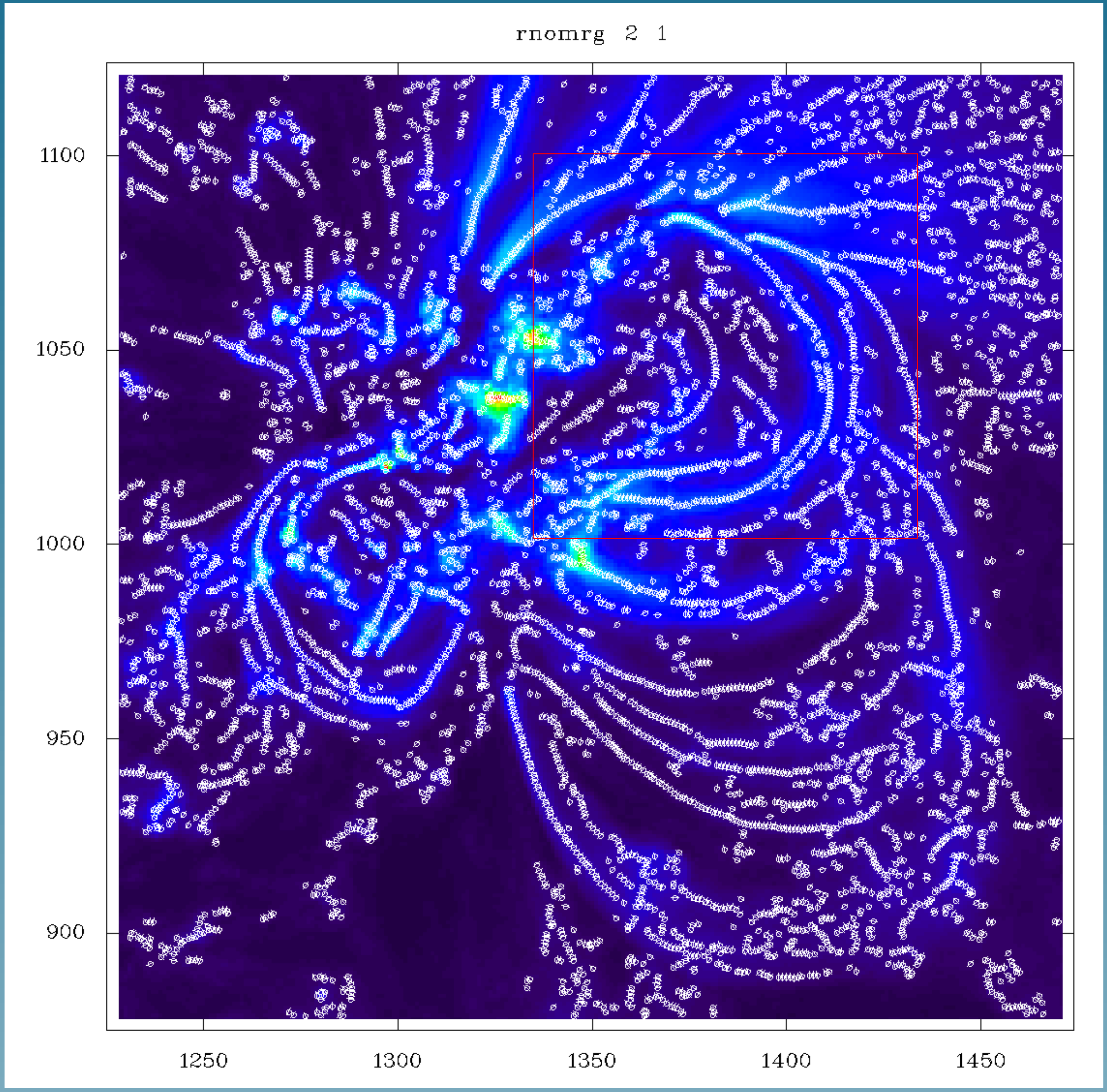

Application to SECCHI EUVI images

Ridgel chains resulting fom the connection step

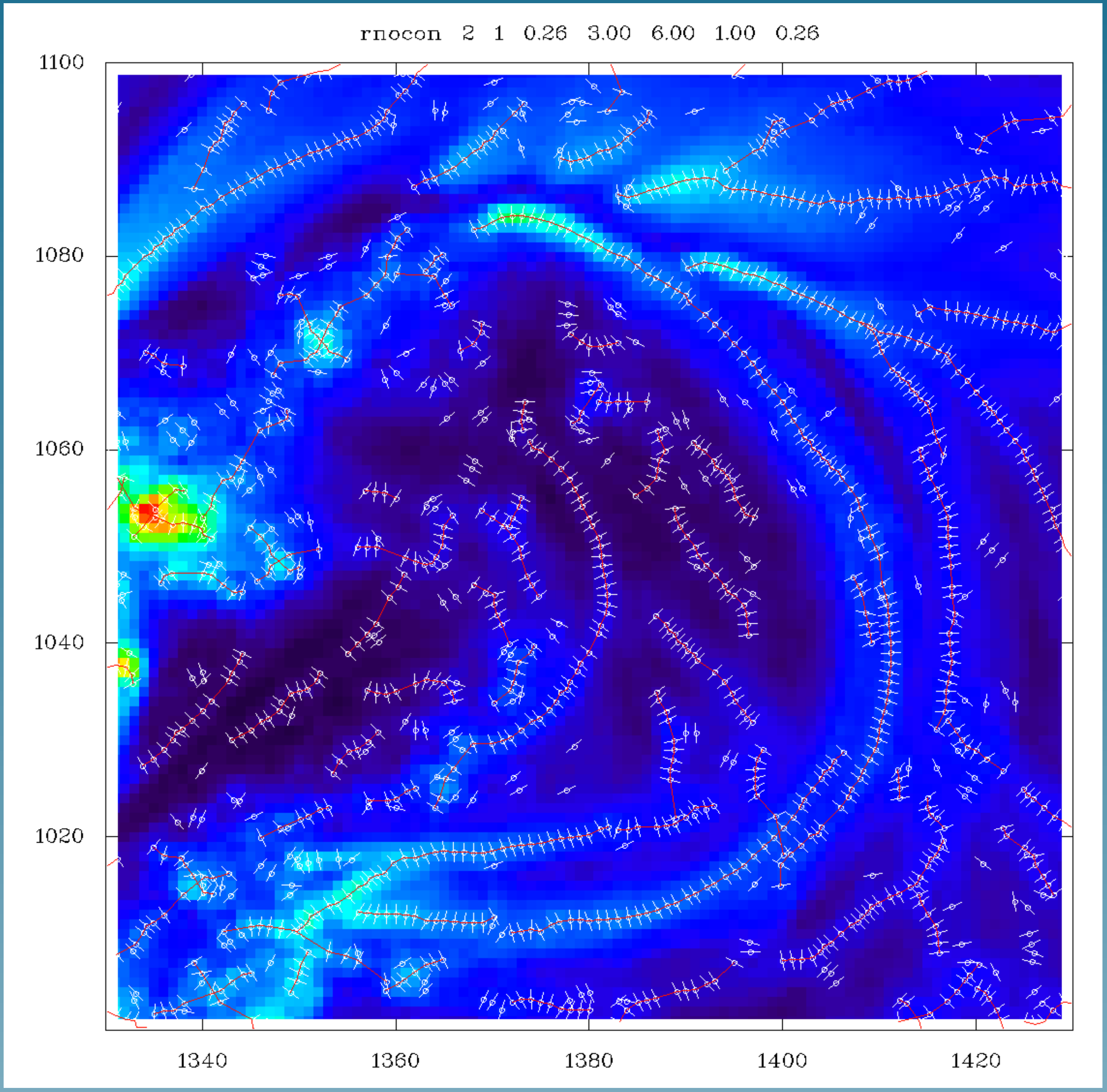

Application to SECCHI EUVI images

First fits to the ridgel chains . . .

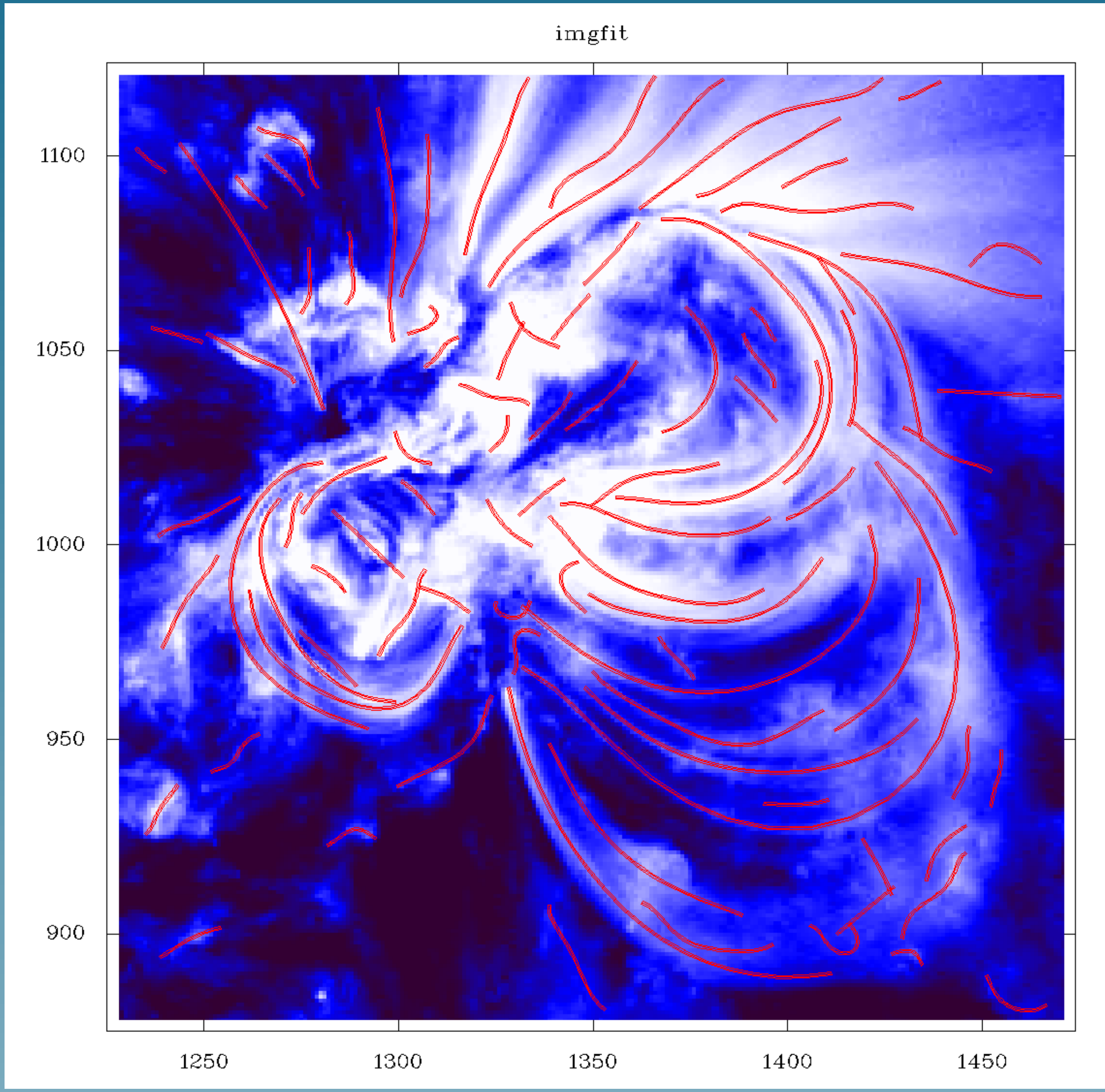

Application to SECCHI EUVI images

. . . after some polishing

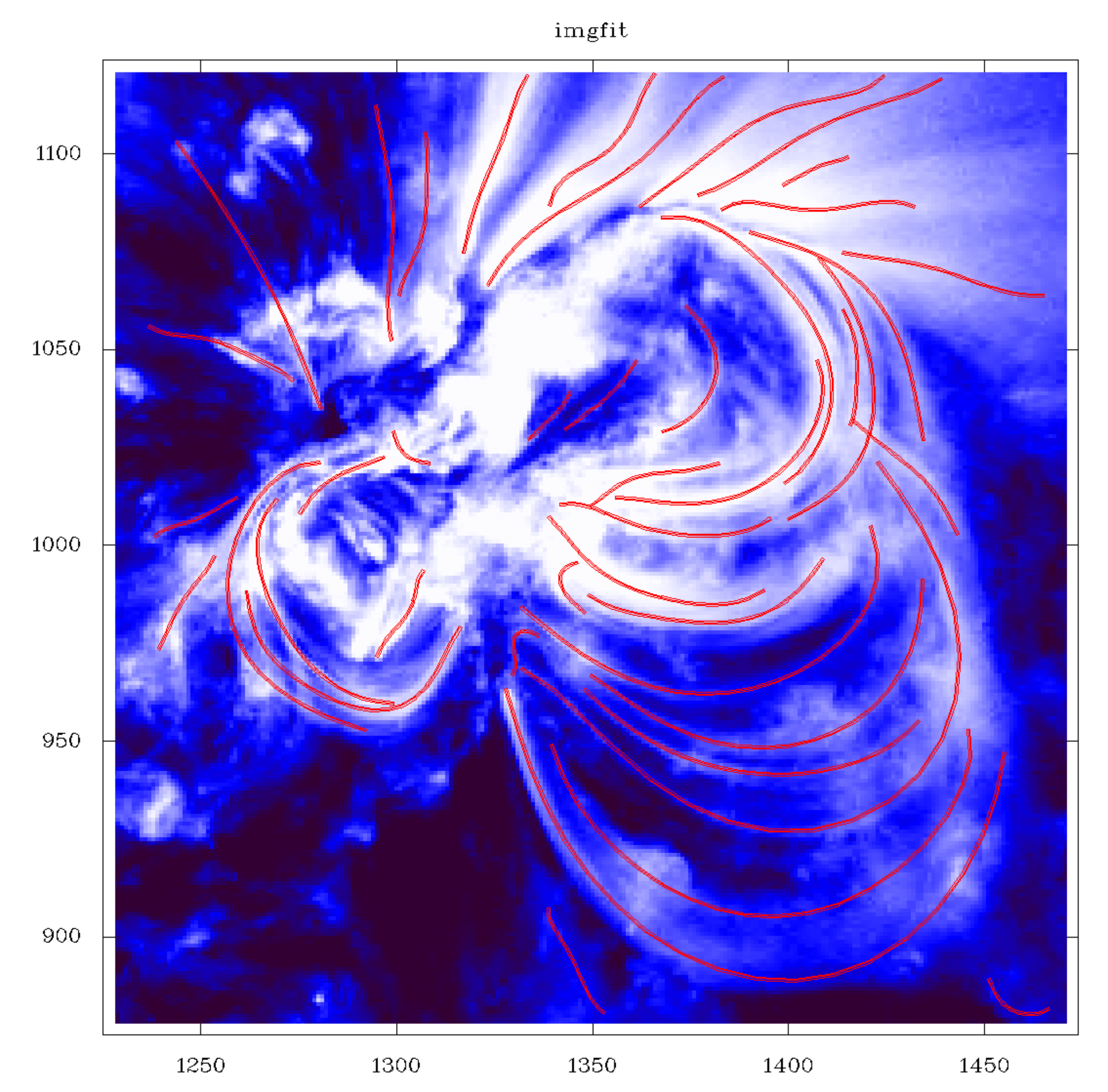

What is SERALD good for ?

- Trace apparent motion of loops (oscillations)

What is SERALD good for ?

- Trace apparent motion of loops (oscillations)
- Comparison with projected field lines from magnetic field models

What is SERALD good for ?

- Trace apparent motion of loops (oscillations)
- Comparison with projected field lines from magnetic field models
- Stereoscopy:

What is SERALD good for ?

- Trace apparent motion of loops (oscillations)
- Comparison with projected field lines from magnetic field models
- Stereoscopy:

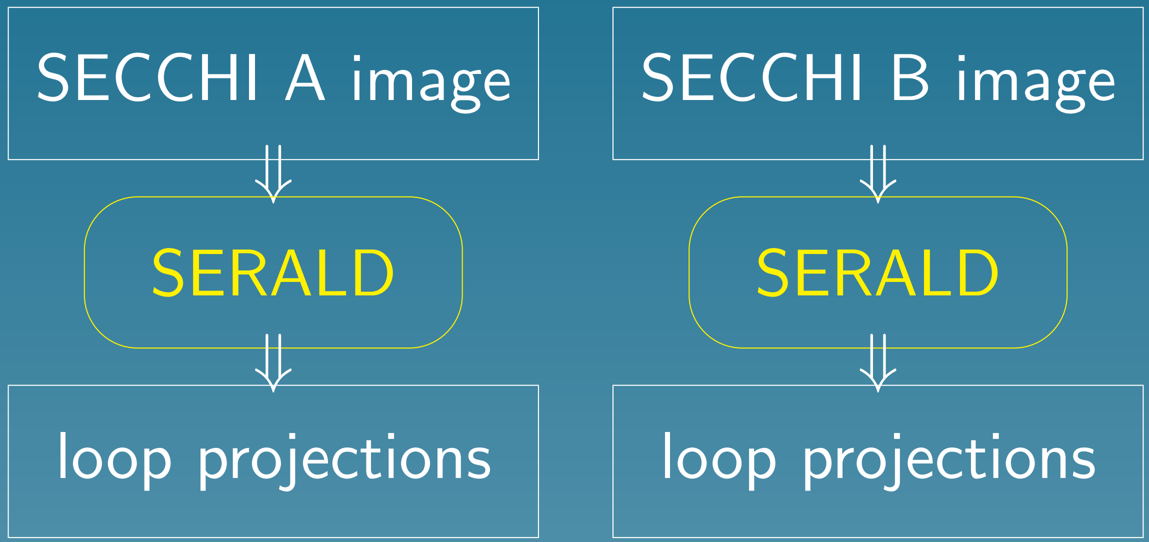

What is SERALD good for ?

- Trace apparent motion of loops (oscillations)
- Comparison with projected field lines from magnetic field models
- Stereoscopy:

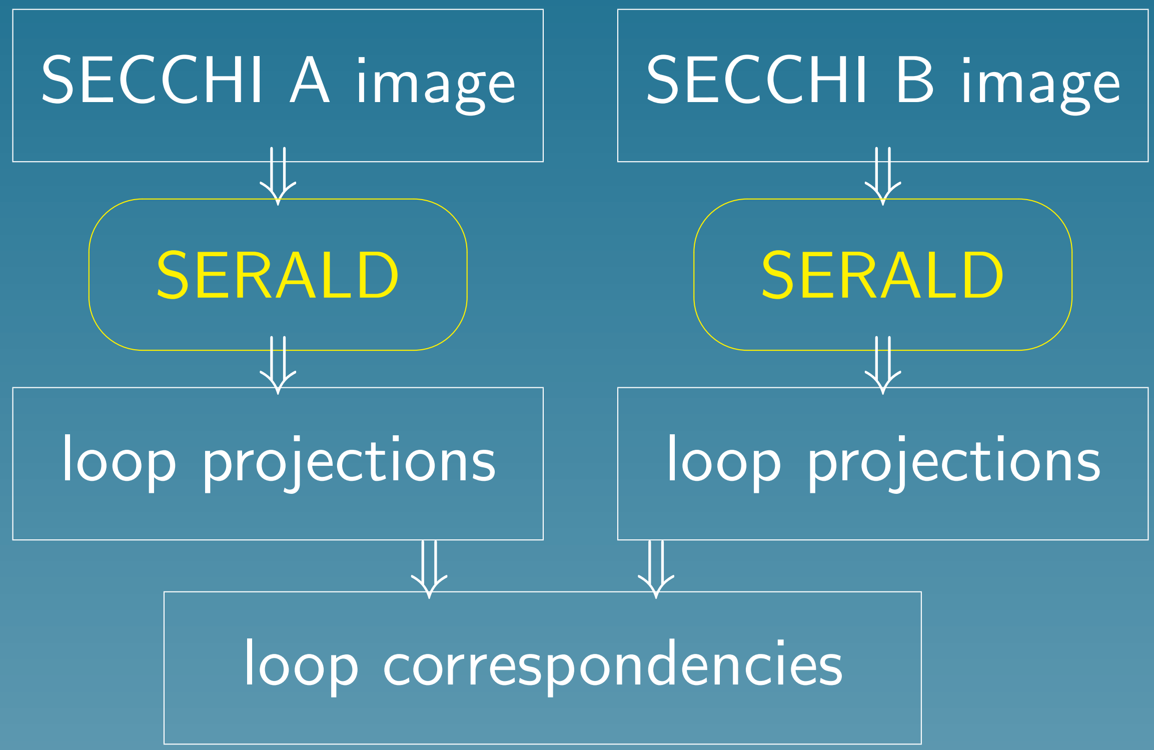

What is SERALD good for ?

- Trace apparent motion of loops (oscillations)
- Comparison with projected field lines from magnetic field models
- Stereoscopy:

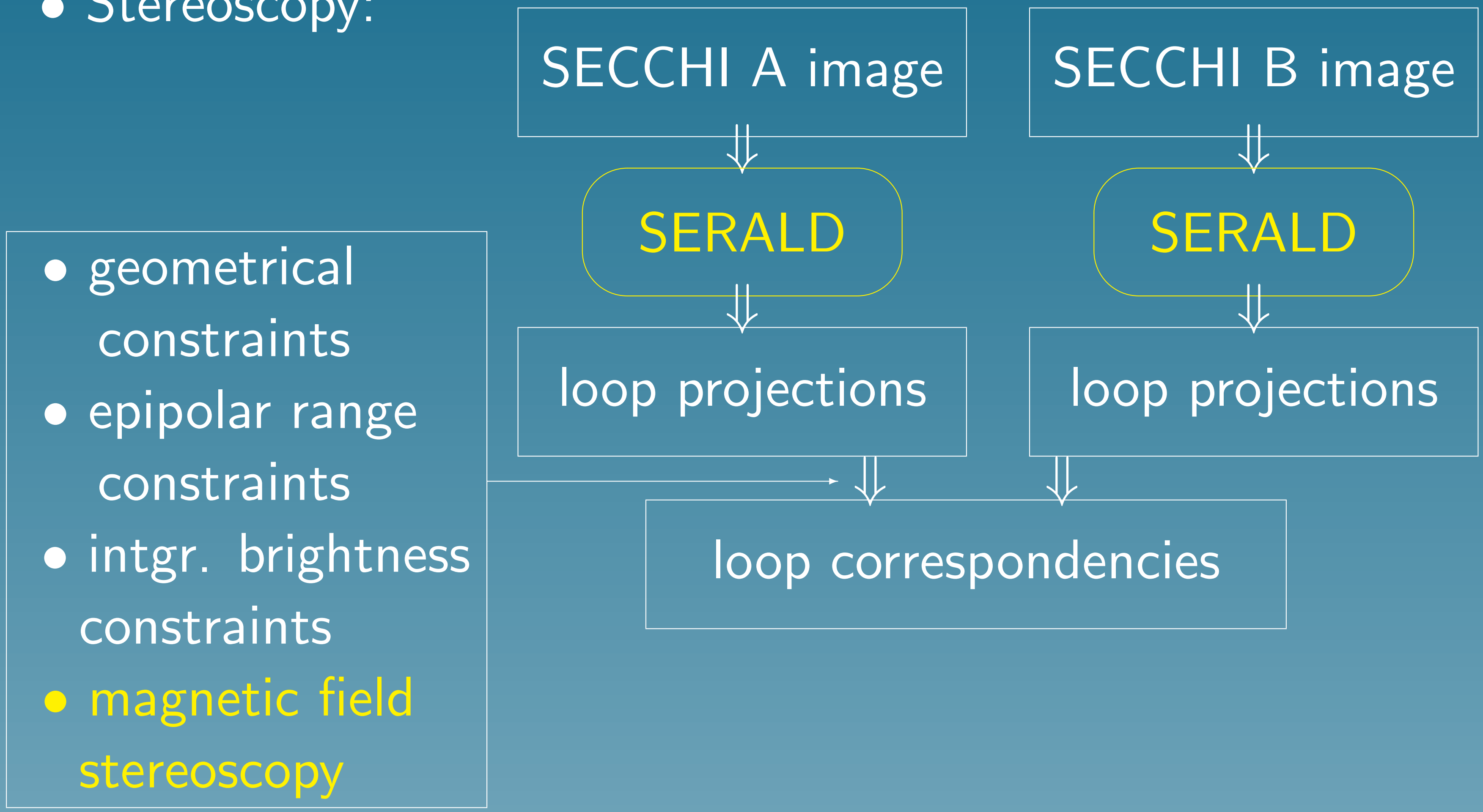

What is SERALD good for ?

- Trace apparent motion of loops (oscillations)
- Comparison with projected field lines from magnetic field models
- Stereoscopy:

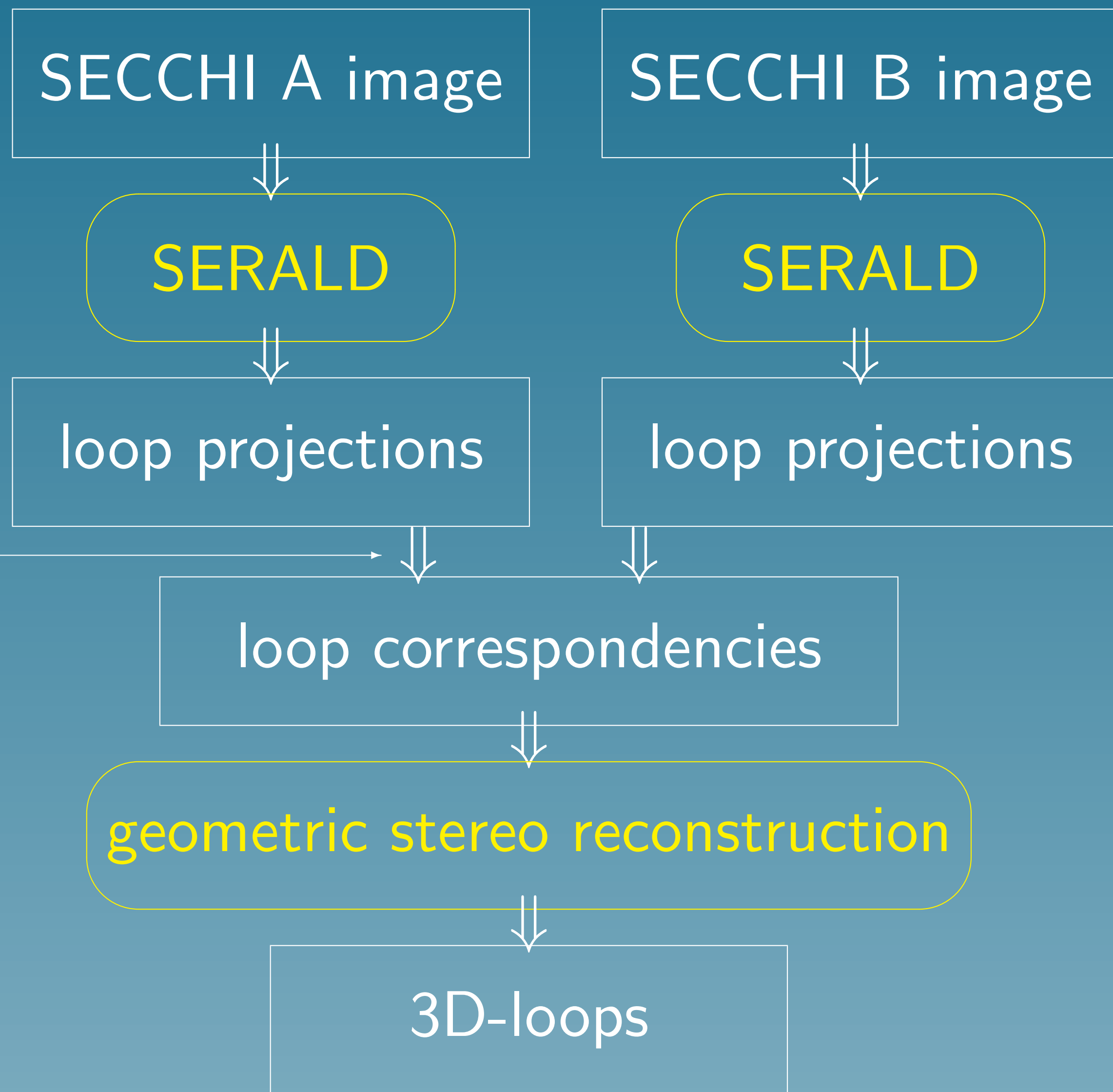

- geometrical constraints
- epipolar range constraints
- intgr. brightness constraints
- magnetic field stereoscopy